上海交通大学
SHANGHAI JIAO TONG UNIVERSITY

Institute of Media, Information, and Network

Multiscale Geometry Analysis

Hongkai Xiong

熊红凯

http://min.sjtu.edu.cn

Department of Electronic Engineering

Shanghai Jiao Tong University

Multiscale Geometry Analysis

1. Directional Wavelet
2. Curvelet
3. Contourlet
4. Bandelet

Wavelet Transform

Fast 2D wavelet transform

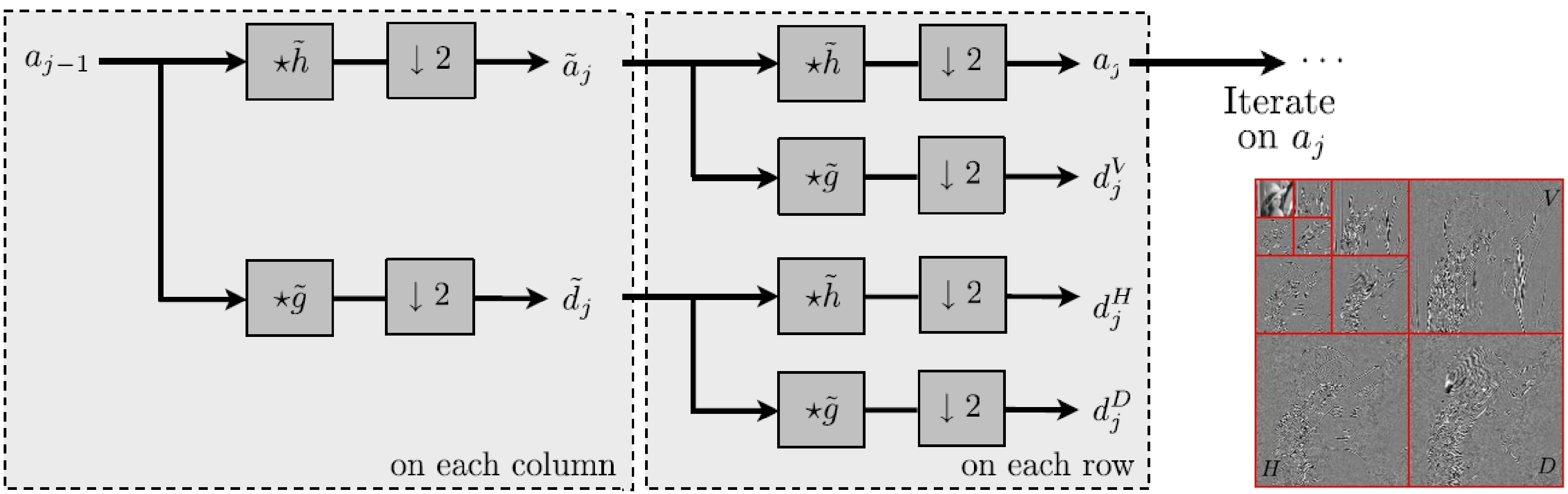

Wavelet Transform

Inverse 2D wavelet transform

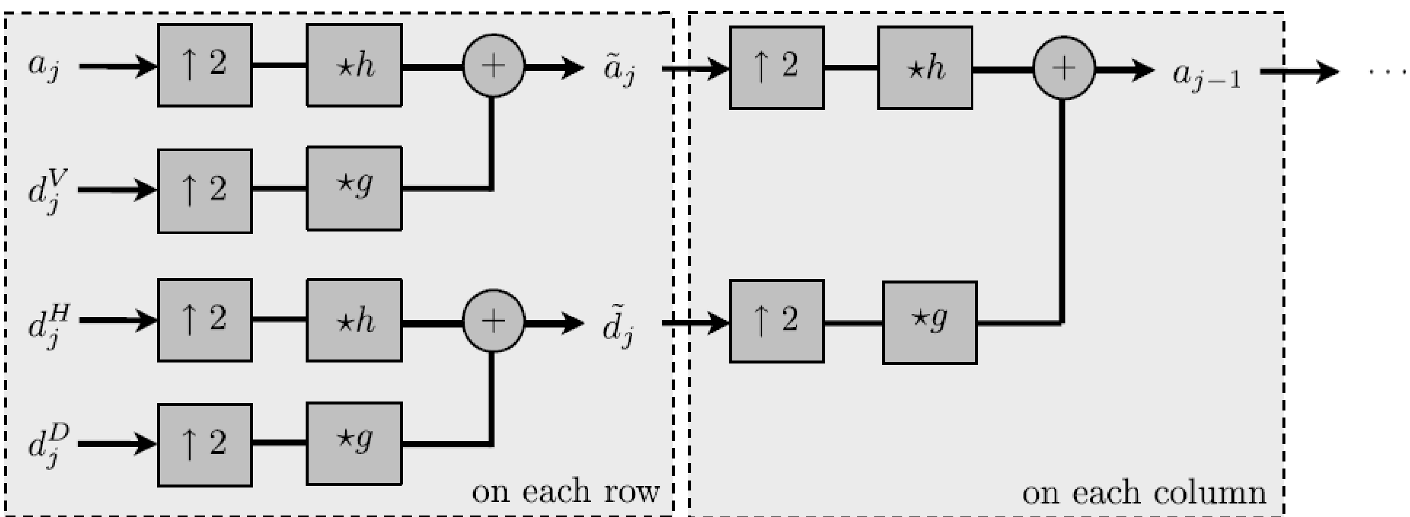

Stable Analysis and Synthesis Operators

wavelets and scaling functions

- To reveal geometric image properties, wavelet frames are constructed with mother wavelets having a direction selectivity, providing information on the direction of sharp transitions such as edges and textures.

- Wavelet frames yield high-amplitude coefficients in the neighborhood of edges, and cannot take advantage of their geometric regularity to improve the sparsity of the representation.

- Frames are potentially redundant and thus more general than bases, with a redundancy measured by frame bounds. They provide the flexibility needed to build signal representations with unstructured families of vectors.

Directional Wavelet Frames

Directional Vanishing Moment

- A directional wavelet $\psi^{\alpha}(x)$ with $x = (x_1, x_2) \in \mathbb{R}^2$ of angle α is a vavelet having p directional vanishing moments along any one-dimensional line of direction $\alpha + \frac{\pi}{2}$ in the plane:

$$\forall \rho \epsilon \mathbb{R}, \int \psi^{\alpha}(\rho \cos \alpha - u \sin \alpha, \rho \sin \alpha + u \cos \alpha) u^k du = 0 \quad \text{for } 0 \leq k \leq p,$$

but does not have directional vanishing moments along the direction α.

- Directional wavelets may be derived by rotating a single mother wavelet $\psi(x_1, x_2)$ having vanishing moments in the horizontal direction, with a rotation operator R_α of angle α in $\mathbb{R}^2$.

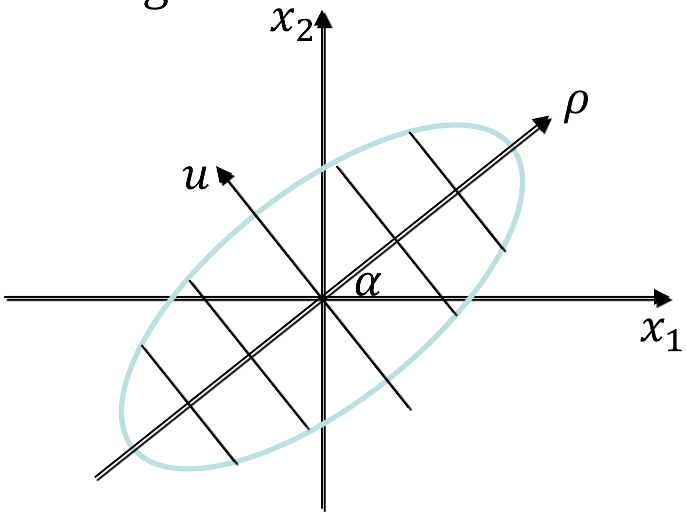

$$\begin{cases} x_1 = \rho \cos \alpha - u \sin \alpha \\ x_2 = \rho \sin \alpha + u \cos \alpha \end{cases}$$

Directional Wavelet Frames

Ridgelet Transform

- To overcome the weakness of wavelets in higher dimensions, Candes and Donoho proposed *ridgelets* which deal effectively with line singularieies in 2-D.

wavelet

$$\psi_{u,s}(t) = \frac{1}{\sqrt{s}}\psi\left(\frac{t-u}{s}\right)$$

$$t = x_1 \cos\theta + x_2 \sin\theta$$

Ridgelet

$$\psi_{u,s,\theta}(x) = \frac{1}{\sqrt{s}}\psi\left(\frac{x_1\cos\theta + x_2\sin\theta - u}{s}\right)$$

Ridgelet transform

$$CRTf(u,s,\theta) = \iint f(x)\psi_{u,s,\theta}(x)dx$$

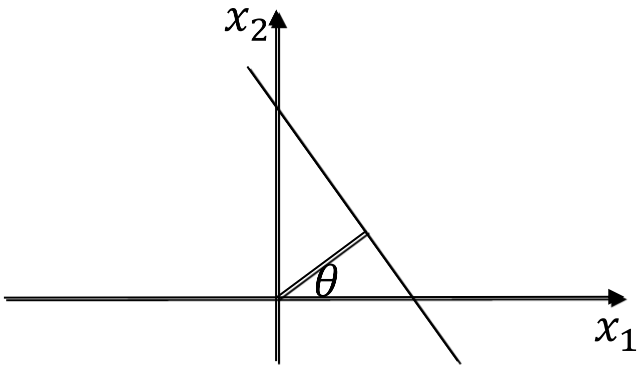

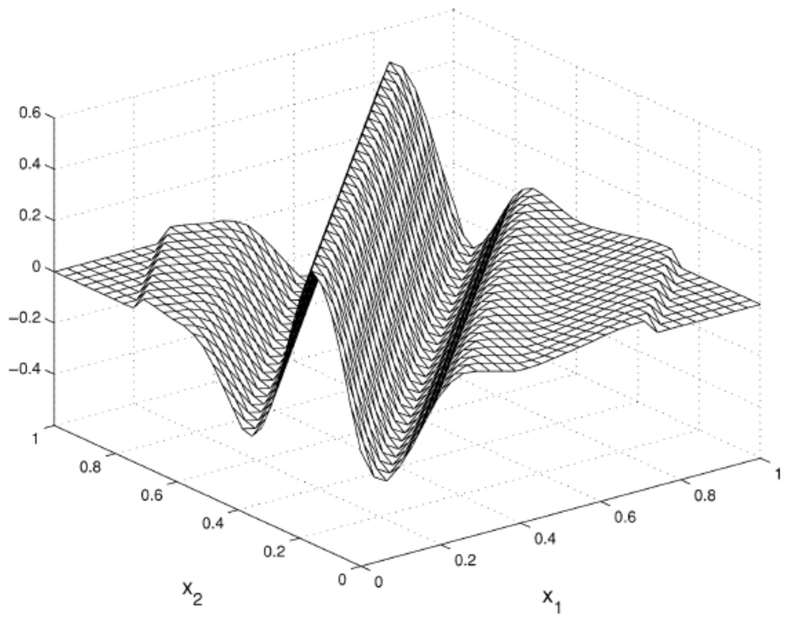

- Ridgelet function which is oriented at an angle θ is constant along the lines $x_1 \cos\theta + x_2 \sin\theta = const$

Directional Wavelet Frames

Ridgelet Transform

- In 2-D, points and lines are related via the Radon transform, thus the wavelet and ridgelet transform are linked via the Radon transform.

Ridgelet transform

$$CRTf(u,s,\theta) = \iint f(x)\psi_{u,s,\theta}(x)dx$$

Radon transform

$$Rf(\theta,t) = \iint f(x)\delta(x_1\cos\theta + x_2\sin\theta - t)dx$$

Ridgelet transform

$$CRTf(u,s,\theta) = \int \psi_{u,s}(t)Rf(\theta,t)dt$$

- Ridget transform can be calculated by applying 1-D wavelet transform to Radon transform $Rf(\theta,t)$ along t.
- $Rf(\theta,t)$ can be obtained from the *projection-slice* theorem.

Directional Wavelet Frames

Ridgelet Transform

- the Radon transform can be obtained by applying the 1-D inverse Fourier transform to the 2-D Fourier transform restricted to radial lines going through the origin.

$$\int e^{-i\xi t} Rf(\theta,t)dt \qquad \text{Fourier transform of } Rf(\theta,t)$$

$$= \int e^{-i\xi t}\left[\iint f(x)\delta(x_1\cos\theta + x_2\sin\theta - t)dx\right]dt$$

$$= \iint f(x)\left[\int e^{-i\xi t}\delta(x_1\cos\theta + x_2\sin\theta - t)dt\right]dx$$

$$= \iint f(x)e^{-i\xi(x_1\cos\theta + x_2\sin\theta)}dx$$

$$= \iint f(x)e^{-ix_1(\xi\cos\theta) - ix_2(\xi\sin\theta)}dx$$

$$= F(\xi\cos\theta, \xi\sin\theta)$$

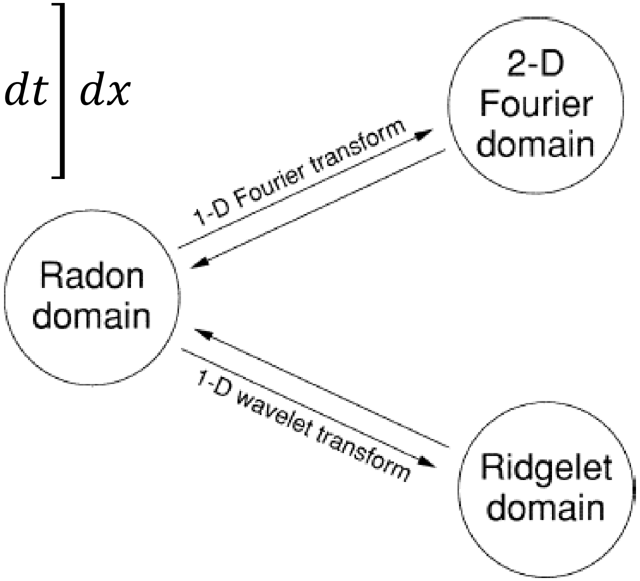

Directional Wavelet Frames

Ridgelet Transform

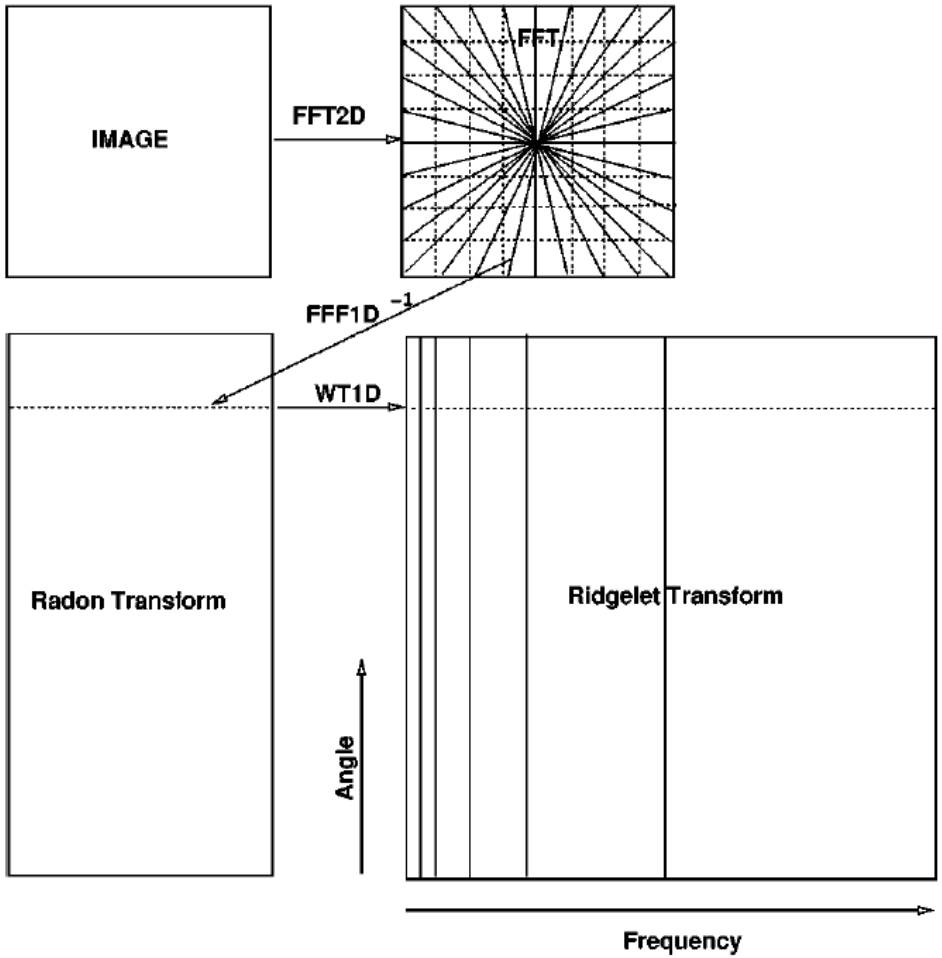

Fig. 2. Ridgelet transform flowgraph. Each of the $2n$ radial lines in the Fourier domain is processed separately. The 1-D inverse FFT is calculated along each radial line followed by a 1-D nonorthogonal wavelet transform. In practice, the 1-D wavelet coefficients are directly calculated in the Fourier space.

Directional Wavelet Frames

Dyadic directional wavelet transform

$$\psi_{u,s}(t) = \frac{1}{\sqrt{s}}\psi\left(\frac{t-u}{s}\right) \xrightarrow{s=2^j} \mathcal{D} = \left\{\psi_{u,2^j}(t) = \frac{1}{\sqrt{2^j}}\psi\left(\frac{t-u}{2^j}\right)\right\}_{u\in\mathbb{R},j\in\mathbb{Z}}$$

wavelets — Translation-invariant wavelet dictionaries

- 1-D dyadic wavelet transform: $Wf(u,2^j) = \langle f, \psi_{u,2^j}\rangle = f * \overline{\psi}_{2^j}(u)$

$$\psi^{\alpha}_{u,s}(x) = \frac{1}{\sqrt{s}}\psi^{\alpha}\left(\frac{x-u}{s}\right) \xrightarrow[\theta = k\pi/K]{s=2^j} \mathcal{D} = \left\{\psi^{\alpha}_{u,2^j}(x) = \frac{1}{2^j}\psi^{\alpha}\left(\frac{x-u}{2^j}\right)\right\}_{u\in\mathbb{R}^2,\alpha\in\Theta,j\in\mathbb{Z}}$$

Directional wavelets — Translation-invariant directional wavelet dictionaries

- Dyadic directional wavelet transform: $Wf(u,2^j,\alpha) = \left\langle f, \psi^{\alpha}_{u,2^j}\right\rangle = f * \bar{\psi}^{\alpha}_{2^j}(u)$

Directional Wavelet Frames

Dyadic directional wavelet transform

$$Wf(u,2^j,\alpha) = \left\langle f, \psi^{\alpha}_{u,2^j} \right\rangle = f * \bar{\psi}^{\alpha}_{2^j}(u)$$

- A wavelet $\psi^{\alpha}_{2^j}(x-u)$ has a support dilated by 2^j, located in the neighborhood of u and oscillates in the direction of $\alpha + \frac{\pi}{2}$.
- If $f(x)$ is constant over the support of $\psi^{\alpha}_{u,2^j}$ along lines of direction $\alpha + \frac{\pi}{2}$, then $\left\langle f, \psi^{\alpha}_{u,2^j} \right\rangle = 0$ because of its directional vanishing moments.
- In particular, this coefficient vanishes in the neighborhood of an edge having a tangent in the direction $\alpha + \frac{\pi}{2}$
- If the edge angle deviates from $\alpha + \frac{\pi}{2}$, then it produces large amplitude coefficients, with a maximum typically when the edge has a direction α.
- Thus, the amplitude of wavelet coefficients depends on the local orientation of the image structures.

Directional Wavelet Frames

Gabor Wavelets

- Gabor wavelet: $\psi^{\alpha}(x_1, x_2) = g(x_1, x_2)e^{-i\eta(-x_1 \sin\alpha + x_2 \cos\alpha)}$

  Gaussian window: $g(x_1, x_2) = \frac{1}{2\pi} e^{-(x_1^2 + x_2^2)/2}$

- Fourier transform: $\bar{\psi}^{\alpha}(\omega_1, \omega_2) = g(\omega_1 + \eta \sin\alpha, \omega_2 - \eta \cos\alpha)$

  $$\bar{\psi}^{\alpha}_{2^j}(\omega_1, \omega_2) = \sqrt{2^j} g(2^j \omega_1 + \eta \sin\alpha, 2^j \omega_2 - \eta \cos\alpha)$$

- In the Fourier plane, the energy of this Gabor wavelet is mostly concentrated around $(-\frac{\eta \sin\alpha}{2^j}, \frac{\eta \cos\alpha}{2^j})$, in a neighborhood proportional to $\frac{1}{2^j}$.

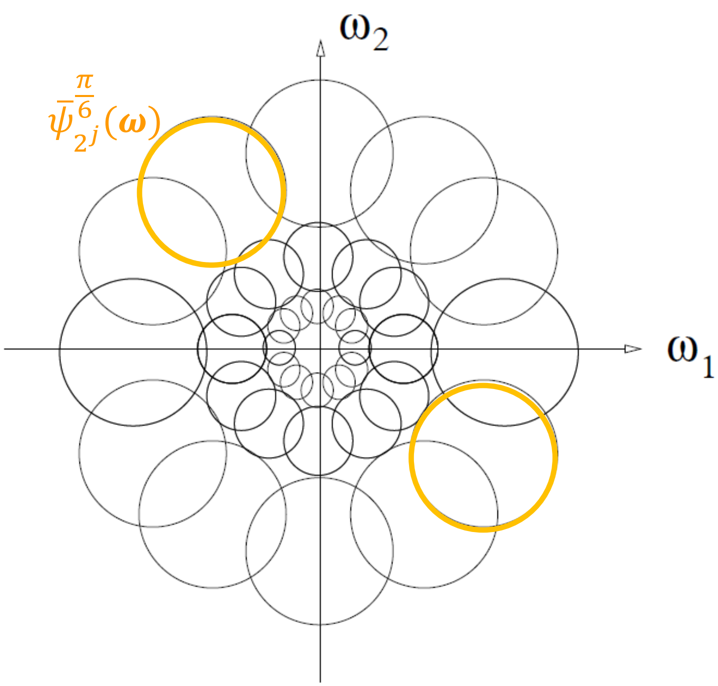

Directional Wavelet Frames

Gabor Wavelets

- The wavelet transform energy $|Wf(u, 2^j, \alpha)|^2$ is large when the angle α and scale 2^j match the direction and scale of high-energy texture components in the neighborhood of u.

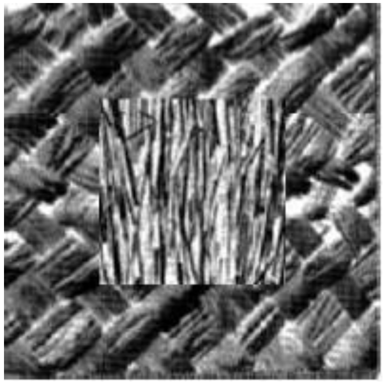

$|Wf(u, 2^{-5}, \pi/2)|^2$

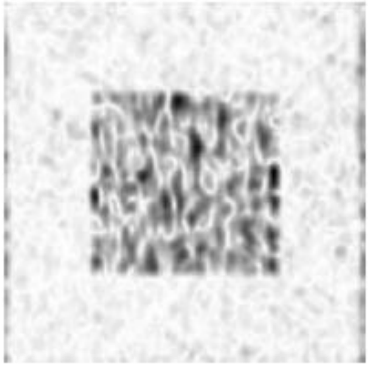

$|Wf(u, 2^{-5}, 0)|^2$

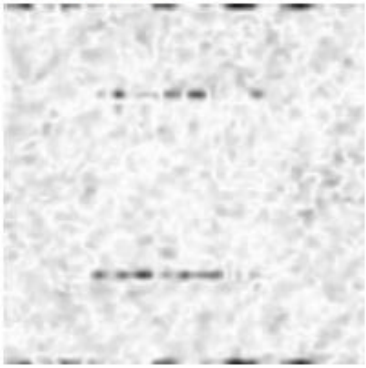

$|Wf(u, 2^{-4}, \pi/2)|^2$

$|Wf(u, 2^{-4}, 0)|^2$

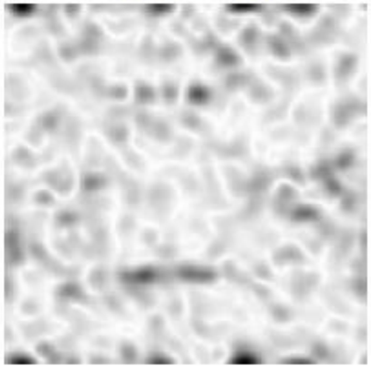

Directional Wavelet Frames

Gabor Wavelets

- A translation-invariant wavelet transform $Wf\left(u,2^{j},\alpha\right)$ for all scales 2^{j} , and angle α requires a large amount of memory. To reduce computation and memory storage, the translation parameter is discretized.

Translation-invariant directional wavelet dictionaries

$$\mathcal{D}=\left\{\psi_{u,2^{j}}^{\alpha}(x)=\frac{1}{2^{j}}\psi^{\alpha}\left(\frac{x-u}{2^{j}}\right)\right\}_{u\epsilon\mathbb{R}^{2},\alpha\in\Theta\, j\epsilon\mathbb{Z}}$$

$$\Big\downarrow\; u=u_{0}2^{j}n$$

$$\mathcal{D}=\left\{\psi_{2^{j}}^{\alpha}(x-u)=\frac{1}{2^{j}}\psi^{\alpha}\left(\frac{x-u_{0}2^{j}n}{2^{j}}\right)\right\}_{n\epsilon\mathbb{Z}^{2},\alpha\in\Theta\, j\epsilon\mathbb{Z}}$$

Curvelet

Dyadic Curvelet Transform

- Curvelet frames were introduced by Candes and Donoho to construct sparse representation for images including edges that are geometrically regular.
- Similarity to wavelet: curvelet frames are obtained by rotating, dilating, and translating elementary waveforms.
- Difference: curvelets have a highly elongated support obtained with a parabolic scaling using different scaling factors along the curvelet width and length.
- These anisotropic waveforms have a much better direction sensitivity than directional wavelets.

Curvelet

First Generation of Curvelets

- First generation of curvelets are based on ridgelets. Applying ridgelet transform to small blocks (a curved edge is almost straight at sufficiently fine scales)

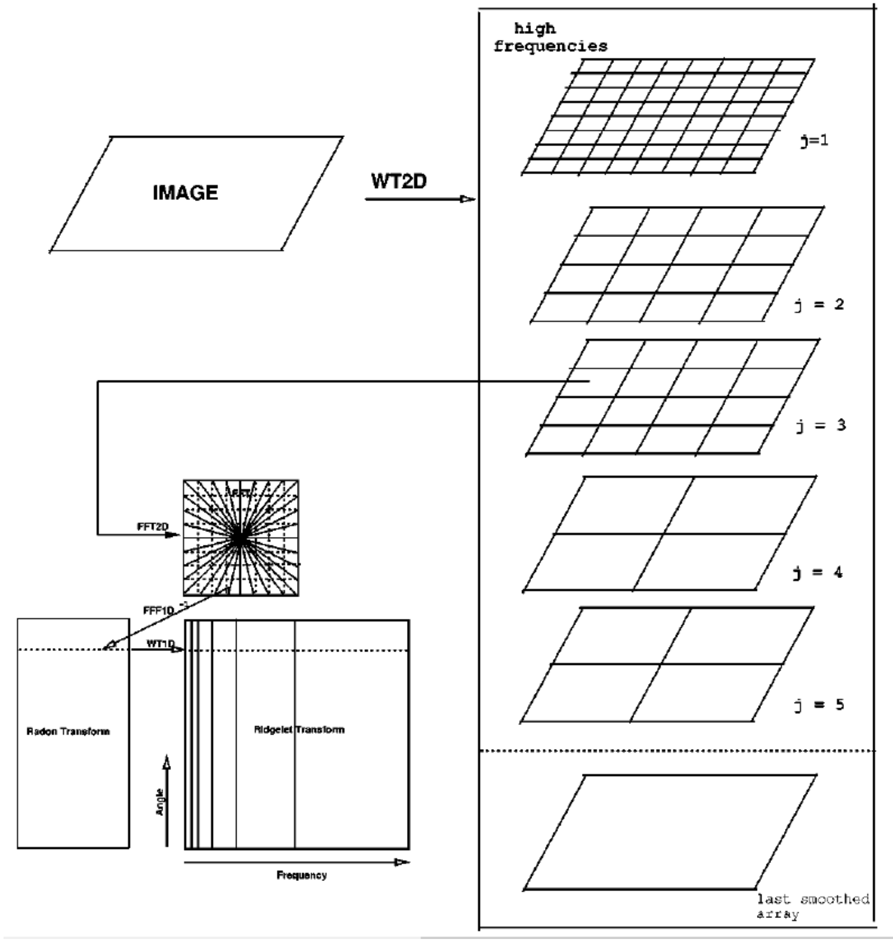

Curvelet

Dyadic Curvelet Transform (Second Generation)

- A curvelet is function $c(x)$ having vanishing moments along the horizontal direction like a wavelet. However, as opposed to wavelets, dilated curvelets are obtained with a *parabolic scaling law* that produces highly elongated waveforms at fine scales:

$$c(x) = c(x_1, x_2)$$

$$\Big\downarrow \text{dilating}$$

$$c_{2^j}(x_1, x_2) = \frac{1}{2^{3j/4}} c\left(\frac{x_1}{2^{j/2}}, \frac{x_1}{2^j}\right)$$

$$\Big\downarrow \text{rotating}$$

$$c_{2^j}^{\alpha}(x) = c_{2^j}(R_\alpha x)$$

$$\Big\downarrow \text{translating}$$

$$c_{u,2^j}^{\alpha}(x) = c_{2^j,u}^{\alpha}(x-u)$$

$$Cf\left(u, 2^j, \alpha\right) = \left\langle f, c_{u,2^j}^{\alpha} \right\rangle = f * \bar{c}\,_{2^j}^{\alpha}(u)$$

$$\psi(x) = c(x_1, x_2)$$

$$\Big\downarrow \text{dilating}$$

$$\psi_{2^j}(x_1, x_2) = \frac{1}{2^j} c\left(\frac{x_1}{2^j}, \frac{x_1}{2^j}\right)$$

$$\Big\downarrow \text{rotating}$$

$$\psi_{2^j}^{\alpha}(x) = \psi_{2^j}(R_\alpha x)$$

$$\Big\downarrow \text{translating}$$

$$\psi_{2^j,u}^{\alpha}(x) = \psi_{u,2^j}^{\alpha}(x-u)$$

$$Wf\left(u, 2^j, \alpha\right) = \left\langle f, \psi_{u,2^j}^{\alpha} \right\rangle = f * \bar{\psi}\,_{2^j}^{\alpha}(u)$$

Curvelet

Dyadic Curvelet Transform

$$c_{2^j}(x_1, x_2) = \frac{1}{2^{3j/4}} c\left(\frac{x_1}{2^{j/2}}, \frac{x_1}{2^j}\right) \qquad \psi_{2^j}(x_1, x_2) = \frac{1}{2^j} c\left(\frac{x_1}{2^j}, \frac{x_1}{2^j}\right)$$

- Curvelet frames were introduced by Candes and Donoho to construct sparse representation for images including edges that are geometrically regular.

- Similarity to wavelet: curvelet frames are obtained by rotating, dilating, and translating elementary waveforms.

- Difference: curvelets have a highly elongated support obtained with a parabolic scaling using different scaling factors along the curvelet width and length.

- These anisotropic waveforms have a much better direction sensitivity than difrectional wavelets.

Curvelet

Dyadic Curvelet Transform

- To obtain a tight frame, the Fourier transform of a curvelet at scale 2^j is defined by

$$\hat{c}_{2^j}(\omega) \stackrel{\text{def}}{=} 2^{3j/4}\hat{\psi}_{2^j}(2^j r)\hat{\phi}\left(\frac{2\theta}{2^{\lfloor j/2 \rfloor}\pi}\right), \text{ with } \omega = r(\cos\theta, \sin\theta)$$

1-D wavelet 1-D angular window

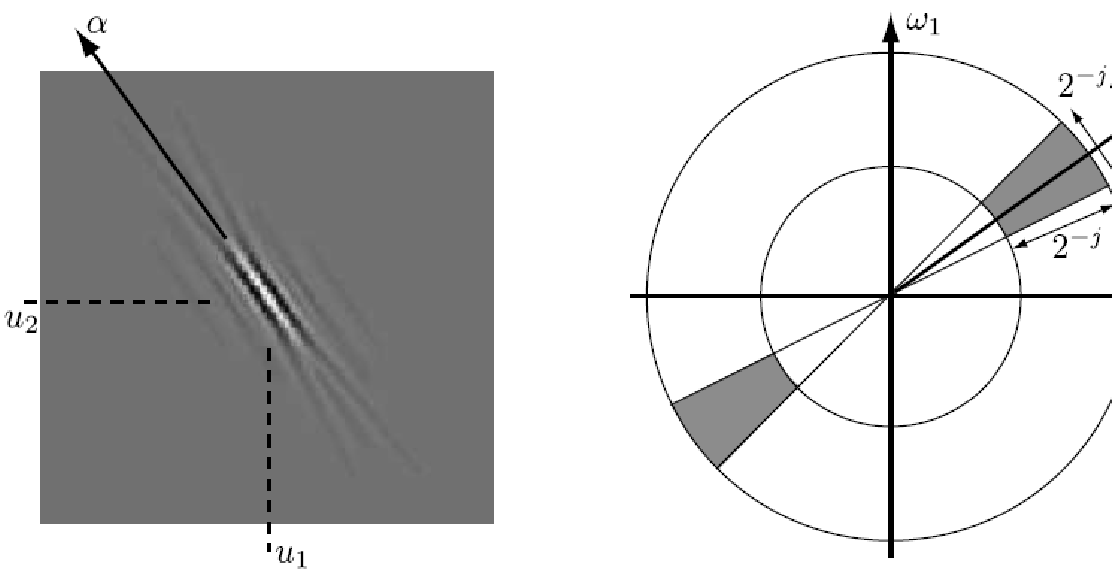

Curvelet

Dyadic Curvelet Transform

- To obtain a tight frame, the Fourier transform of a curvelet at scale 2^j is defined by

$$\hat{c}_{2^j}(\omega) \stackrel{\text{def}}{=} 2^{3j/4}\hat{\psi}(2^j r)\hat{\phi}\left(\frac{2\theta}{2^{\lfloor j/2 \rfloor}\pi}\right), \text{ with } \quad \omega = r(\cos\theta, \sin\theta)$$

1-D wavelet 1-D angular window

- The wavelet $\hat{\psi}$ is chosen to have a compact support in $[\frac{1}{2}, 2]$ and satisfies the dyadic frequency covering:

$$\forall r \epsilon \mathbb{R}^*, \sum_{j=-\infty}^{\infty} \left|\hat{\psi}\left(2^j r\right)\right|^2 = 1$$

- A translation-invariant dyadic curvelet dictionary is a dyadic translation-invariant tight frame that defines a complete and stable signal representation.

Curvelet

Dyadic Curvelet Transform

- To obtain a tight frame, the Fourier transform of a curvelet at scale 2^j is defined by

- **Theorem 1:** (*Candes, Donoho*) For any $f \epsilon \mathbf{L}^2(\mathbb{R}^{\mathbf{2}})\mathbf{Im}\Phi$

$$\|f\|^2 = \sum_{j\epsilon\mathbb{Z}} 2^{-3j/2} \sum_{\alpha\in\Theta_j} \left\|Cf\left(\cdot\,, 2^j, \alpha\right)\right\|^2,$$

and

$$f(x) = \sum_{j\epsilon\mathbb{Z}} 2^{-\frac{3j}{2}} \sum_{\alpha\in\Theta_j} Cf\left(\cdot\,, 2^j, \alpha\right) * c_{2^j}^{\alpha}(x).$$

Curvelet

Curvelet Properties

- Since the Fourier transform $\hat{c}_{2^j}(\omega_1, \omega_2)$ is zero in the neighborhood of the vertical axis $\omega_1 = 0$, $c_{2^j}(x_1, x_2)$ has an infinite number of vanishing moments in the horizontal direction

$$\forall \omega_2, \frac{\partial^q \hat{c}_{2^j}}{\partial^q \omega_2}(0, \omega_2) = 0 \Longrightarrow \forall q \geq 0, \forall x_2, \int c_{2^j}(x_1, x_2) x_1^q \, dx_1 = 0$$

- A rotated curvelet $c^{\alpha}_{u,2^j}$ has vanishing moments in the direction $\alpha + \pi/2$, whereas its support is elongated in the direction α.

Curvelet

Discretization of Translation

- Curvelet tight frames are constructed by sampling the translation parameter u. These tight frames provide sparse representations of signals including regular geometric structures.

$$\mathcal{D} = \left\{c^{\alpha}_{u,2^j}(x)\right\}_{u\epsilon\mathbb{R}^2,\alpha\in\Theta\, j\epsilon\mathbb{Z}}$$

$$\Big\downarrow\; u_m^{(j,\alpha)} = R_\alpha(2^{j/2}m_1, 2^j m_2)$$

$$\mathcal{D} = \left\{c^{\alpha}_{j,m}(x) = c^{\alpha}_{2^j}(x - u_m^{(j,\alpha)})\right\}_{m\epsilon\mathbb{Z}^2,\alpha\in\Theta, j\epsilon\mathbb{Z}}$$

- The curvelet sampling grid depends on the scale 2^j and on the angle α. Sampling intervals are proportional to the curvelet width 2^j in the direction $\alpha + \pi/2$ and to its length $2^{j/2}$ in the direction α.

Curvelet

Discretization of Translation

- The curvelet sampling grid depends on the scale 2^j and on the angle α. Sampling intervals are proportional to the curvelet width 2^j in the direction $\alpha + \pi/2$ and to its length $2^{j/2}$ in the direction α:

$$\forall m = (m_1, m_2) \epsilon \mathbb{Z}^2, \qquad u_m^{(j,\alpha)} = R_\alpha(2^{j/2} m_1, 2^j m_2)$$

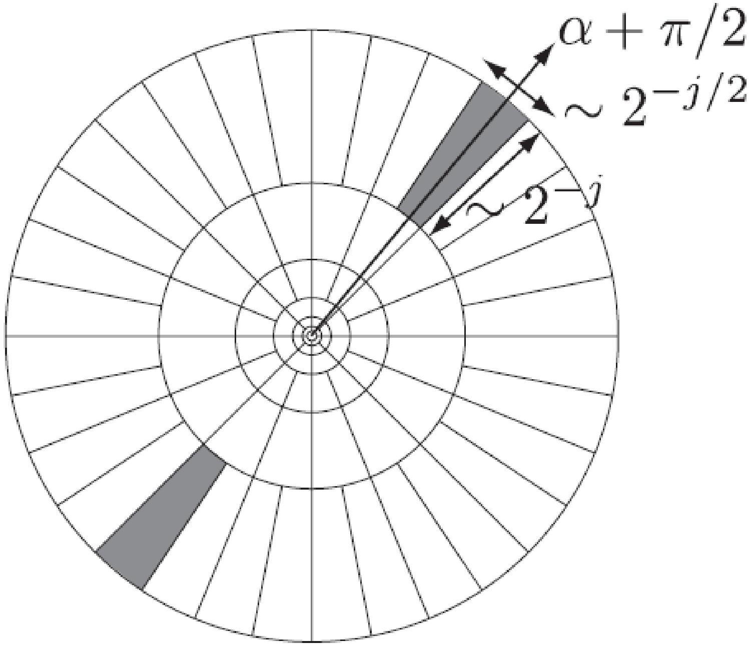

Frequency tiling

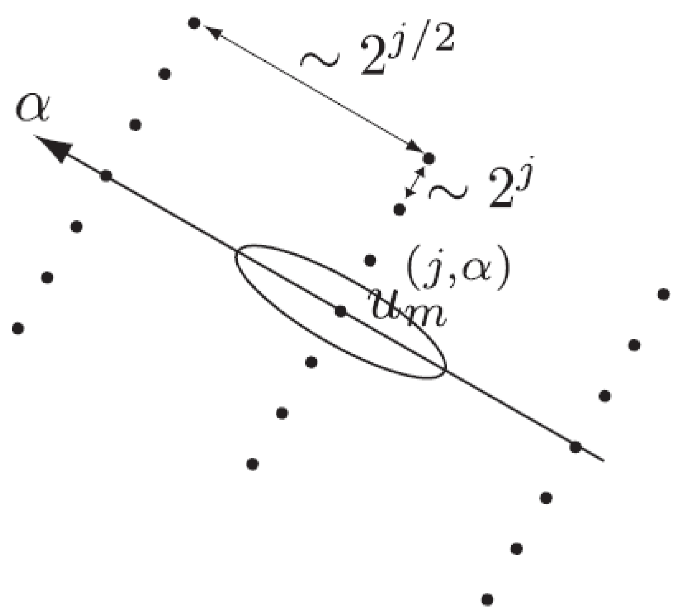

Spatial sampling

Curvelet

Discretization of Translation

- This curvelet family is a tight frame of $\mathbf{L}^2(\mathbb{R}^2)$.

$$\mathcal{D} = \left\{ c_{j,m}^{\alpha}(x) = c_{2^j}^{\alpha}(x - u_m^{(j,\alpha)}) \right\}_{m\epsilon\mathbb{Z}^2, \alpha\in\Theta, j\epsilon\mathbb{Z}}$$

- **Theorem 2:** (*Candes, Donoho*) For any $f \epsilon \mathbf{L}^2(\mathbb{R}^2)$

$$\|f\|^2 = \sum_{j\epsilon\mathbb{Z}} \sum_{\alpha\in\Theta_j} \left| \left\langle f, c_{u,2^j}^{\alpha} \right\rangle \right|^2,$$

and

$$f(x) = \sum_{j\epsilon\mathbb{Z}} \sum_{\alpha\in\Theta_j} \sum_{m\epsilon\mathbb{Z}^2} \left\langle f, c_{u,2^j}^{\alpha} \right\rangle c_{j,m}^{\alpha}(x).$$

Curvelet

Wavelet versus Curvelet Coefficients

- An edge is covered by fewer curvelets than wavelets having a direction equal to the edge direction.

- If the angle α of the curvelet deviates from θ, then curvelet coefficients decay quickly because of the narrow frequency localization of curvelets. This gives a high-directional selectivity to curvelets.

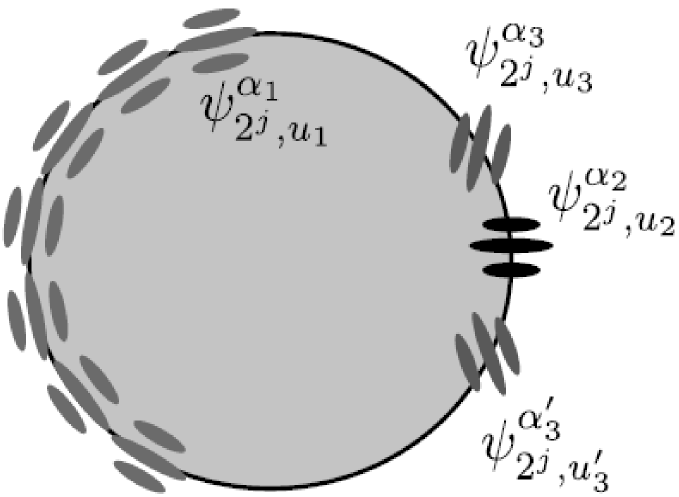

Directional wavelets

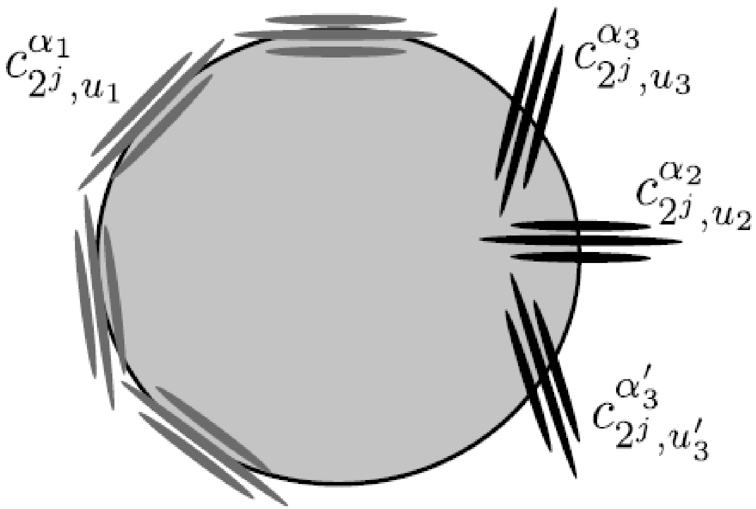

Curvelets

Curvelet

Fast curvelet Decomposition Algorithm

- The fast curvelet transform replaces the polar tiling of the Fourier domain by a recto-polar tiling.

- Computation of the two-dimensional DFT $\hat{f}[k]$ of $f[n]$.
- For each j and the corresponding $2^{-\lfloor j/2 \rfloor+2}$ angles α, calculation of $\hat{f}[k]\hat{c}_j^{\alpha}[-k]$.
- Computation of the inverse Fourier transform of $\hat{f}[k]\hat{c}_j^{\alpha}[-k]$ on the smallest possible warped frequency rectangle including the wedge support of $\hat{c}_j^{\alpha}[-k]$.

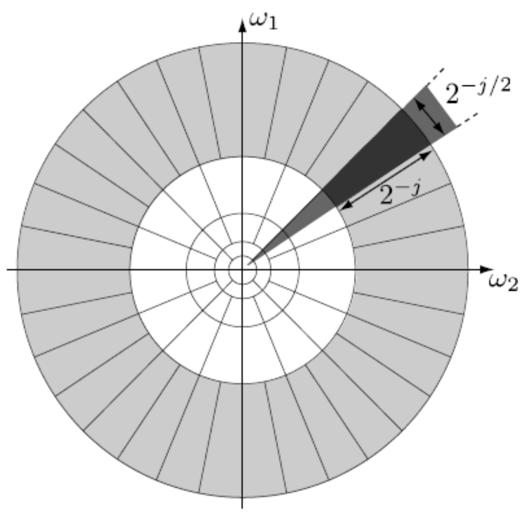

Frequency plane tiling

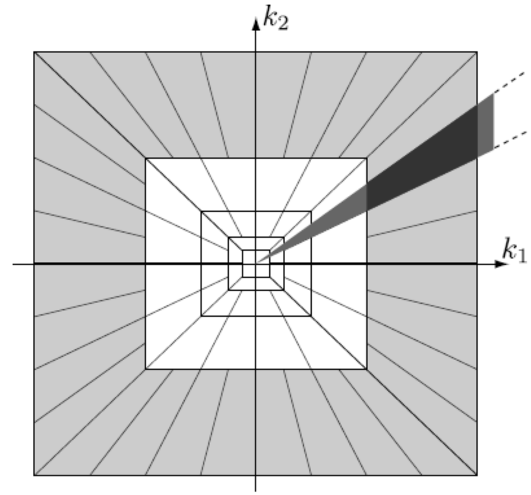

Discrete frequency tiling

Curvelet

Denoising

Fig. 5. (Top left) Noisy image and (top right) filtered images using the decimated wavelet transform, (bottom left) the undecimated wavelet transform and the (bottom right) curvelet transform.

Contourlet

Fast curvelet Decomposition Algorithm

- curvelet constructions require a rotation operation and correspond to a 2-D frequency partition based on the polar coordinate. This makes the curvelet construction simple in the continuous domain but causes the implementation for discrete images—sampled on a rectangular grid—to be very challenging.
- In particular, approaching critical sampling seems difficult in such discretized constructions.

➢ This fact motivates the development of a directional multiresolution transform like curvelets, but directly in the discrete domain, which results in the *contourlet construction.*

➢ The Laplacian pyramid is first used to capture the point discontinuities, and then followed by a directional filter bank (DFB) to link point discontinuities into linear structures.

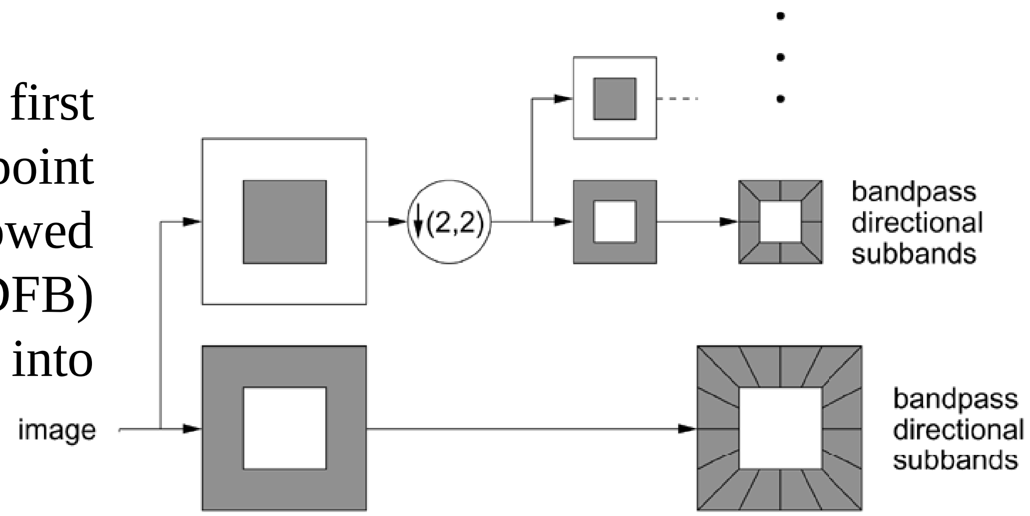

Laplacian Pyramid Directional Filter Banks

Contourlet

Laplacian Pyramid

- The LP decomposition at each level generates a downsampled lowpass version of the original and the difference between the original and the prediction, resulting in a bandpass image. In particular, approaching critical sampling seems difficult in such discretized constructions.

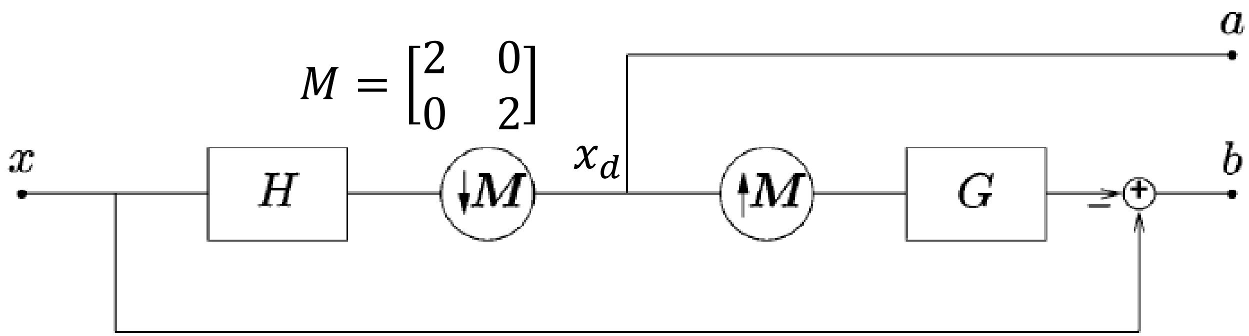

lowpass

bandpass

analysis filter sampling matrix synthesis filter

$$x_d[n_1, n_2] = x[2n_1, 2n_2]$$

$$X_d[\omega_1, \omega_2] = \frac{1}{4}\sum_{j=0}^{1}\sum_{i=0}^{1} X\left(\frac{\omega_1 - 2\pi i}{2}, \frac{\omega_2 - 2\pi j}{2}\right)$$

Contourlet

Traditional 2D filter banks

- **Traditional separable 2D filter banks**

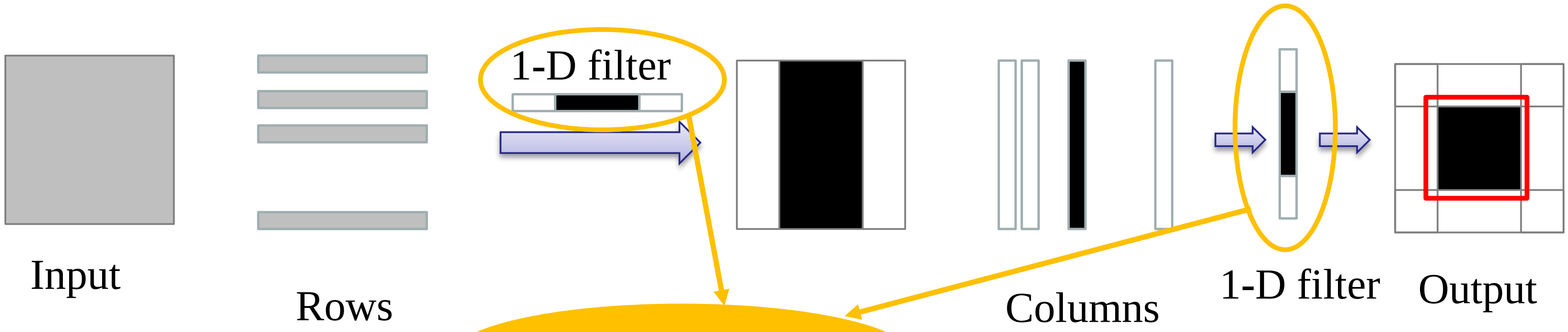

Separable Filters

Diagonal sampling matrix

$$\begin{bmatrix}2 & 0\\ 0 & 1\end{bmatrix}, \quad \begin{bmatrix}1 & 0\\ 0 & 2\end{bmatrix}$$

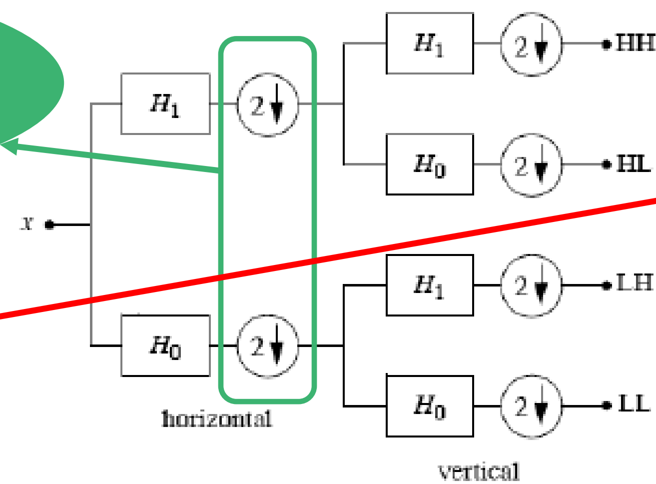

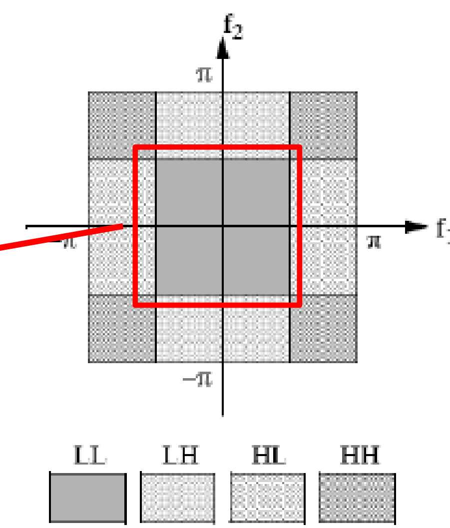

Only Rectangular Shape

Contourlet

Quincunx Filter Bank

- **Traditional Directional Filter Banks**
    - A simple example of 2-channel directional filter banks

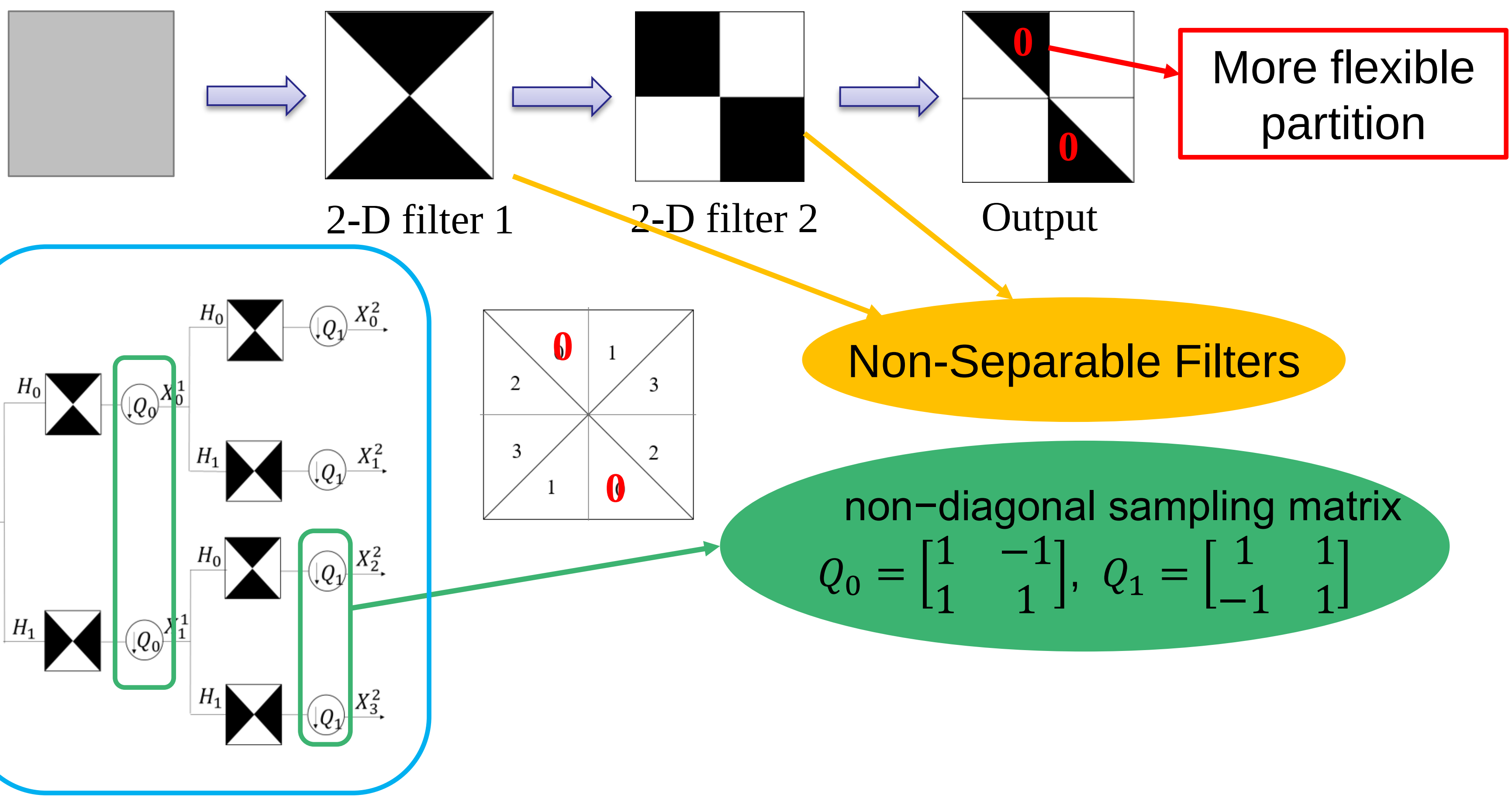

Contourlet

2-D Sampling

- **Example 1:** Sampling matrix $M = \begin{bmatrix} 2 & 1 \\ -1 & 1 \end{bmatrix}$
  - Integer lattice $\Lambda = \mathbb{Z}^2$
  - Sublattice $\Lambda_M = \{Mn: n \in \Lambda\} = \{Mn: n \in \Lambda\}$

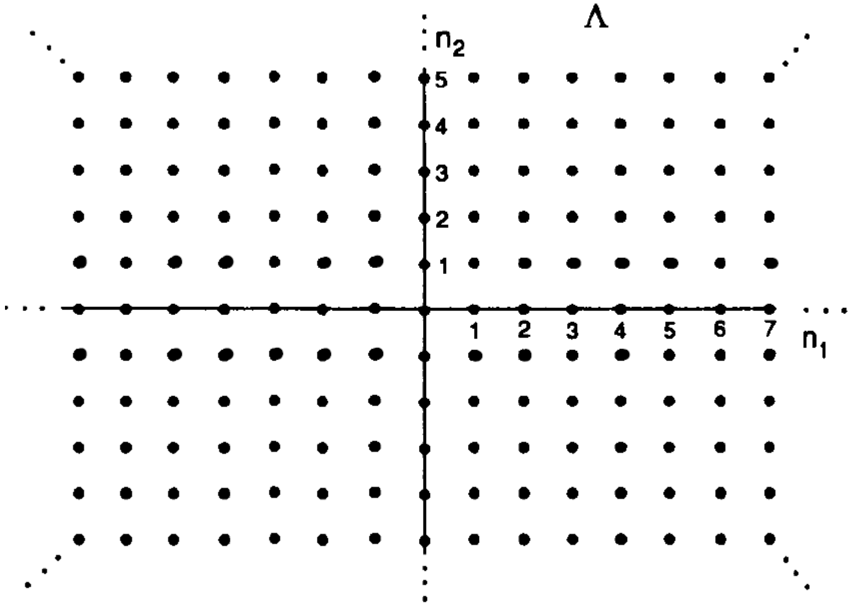

Integer lattice Λ

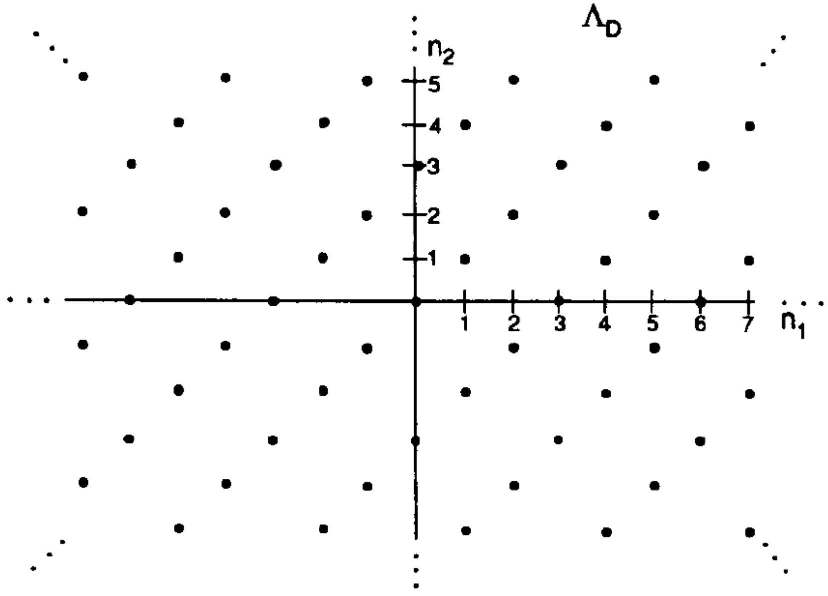

Lattice Λ_M generated by sampling matrix M

Contourlet

2-D Sampling

- **Example 1:** Downsampling with matrix $M = \begin{bmatrix} 2 & 1 \\ -1 & 1 \end{bmatrix}$
  - $Mn = \begin{bmatrix} 2 & 1 \\ -1 & 1 \end{bmatrix} \begin{bmatrix} n_1 \\ n_2 \end{bmatrix} = \begin{bmatrix} 2n_1 + n_2 \\ -n_1 + n_2 \end{bmatrix}$
  - Downsampled signal $x_d[n] = x[Mn]$
  - Downsampled signal in frequency domain $X_d(\omega_1, \omega_2)$?

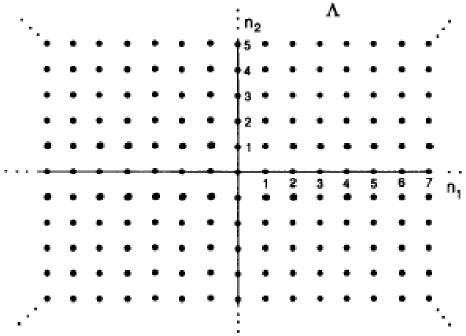

(a)

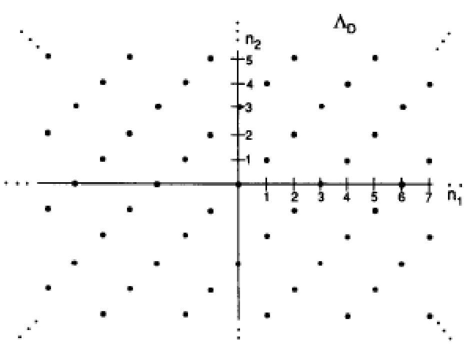

(b)

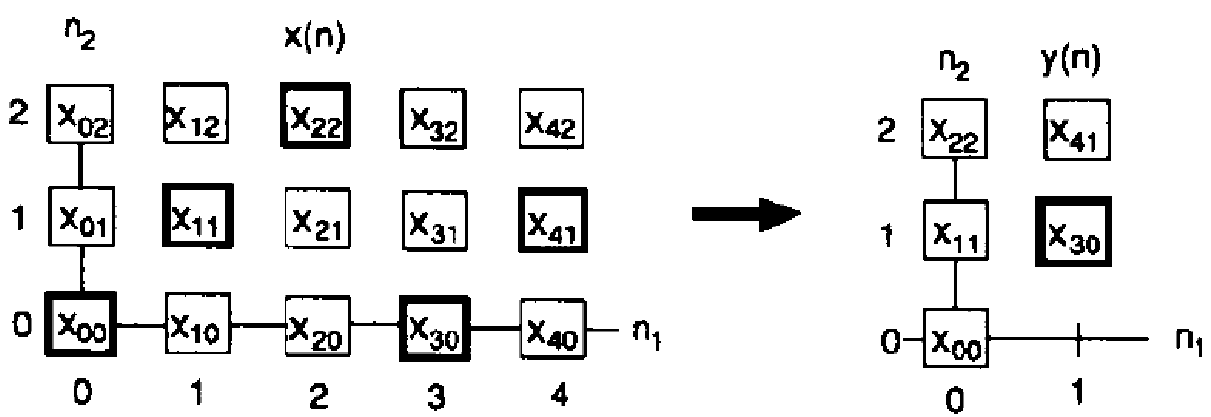

$x_d[1,1] = x[3,0]$

Contourlet

2-D Sampling

- 1-D sampling

$$X_d(\omega) = \frac{1}{M}\sum_{k=0}^{M-1} X\left(\frac{\omega}{M} - \frac{2\pi k}{M}\right)$$

$\omega \in \mathbb{R}, k \in \mathbb{Z}, M \in \mathbb{Z}$

- 2-D sampling

$$\underbrace{X_d(\omega)}_{\text{vector}} = \frac{1}{\underbrace{|\det(M)|}_{\text{Integer matrix}}} \sum_{l=0}^{|\det(M)|-1} X(M^{-T}\omega - 2\pi M^{-T} \underbrace{k_l}_{\text{coset vector}})$$

- **Example 1:** Subsampling with matrix $M = \begin{bmatrix} 2 & 1 \\ -1 & 1 \end{bmatrix}$

➢ $|\det(M)| = 3$

➢ $k_0 = \begin{bmatrix} 0 \\ 0 \end{bmatrix}, k_1 = \begin{bmatrix} 1 \\ 0 \end{bmatrix}, k_0 = \begin{bmatrix} 2 \\ 0 \end{bmatrix}$

Contourlet

2-D Sampling

◆ **Example 1:** Upsampling with matrix $M = \begin{bmatrix} 2 & 1 \\ -1 & 1 \end{bmatrix}$

- $M^{-1} = \frac{1}{3}\begin{bmatrix} 1 & -1 \\ 1 & 2 \end{bmatrix}, M^{-1}n = \frac{1}{3}\begin{bmatrix} n_1 - n_2 \\ n_1 + 2n_2 \end{bmatrix}$
- Upsampled signal $x_u[n] = \begin{cases} x[M^{-1}n], & \text{if } M^{-1}n \in \Lambda \\ 0, & \text{otherwise} \end{cases}$
- Upsampled signal in frequency domain $X_u(\omega_1, \omega_2)$?

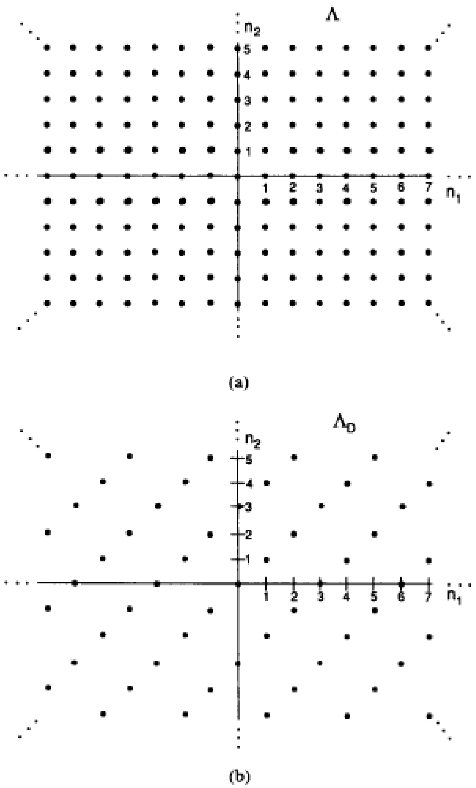

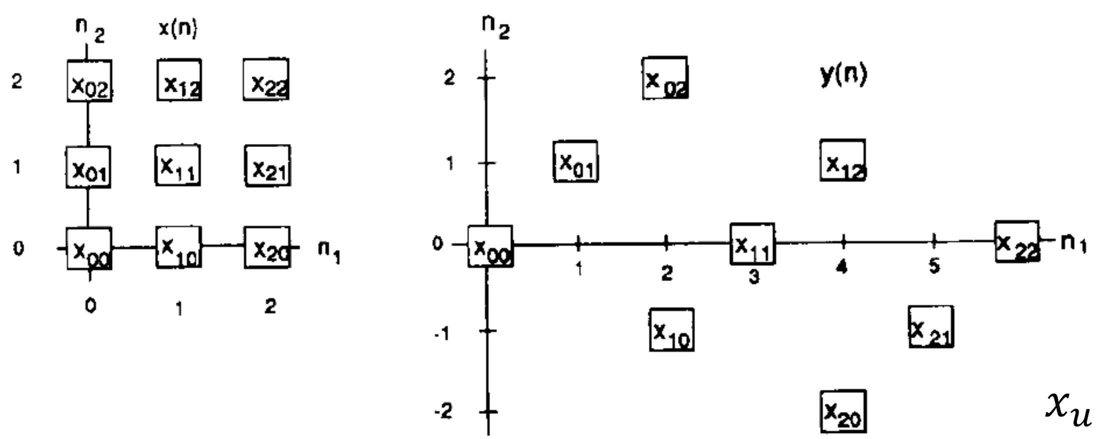

$x_u[3,0] = x[1,1]$

Contourlet

2-D Sampling

- 1-D upsampling

$$X_u(\omega) = X(M\omega)$$

- 2-D upsampling

$$X_u(\omega) = (M^T\omega)$$

- **Example 1:** Upsampling with matrix $M = \begin{bmatrix} 2 & 1 \\ -1 & 1 \end{bmatrix}$

  - $X_u(\omega) = (M^T\omega) = \begin{bmatrix} 2\omega_1 - \omega_2 \\ \omega_1 + \omega_2 \end{bmatrix}$
  - The rectangular spectral region

    $\{-\pi \leq \omega_1 \leq \pi\} \cap \{-\pi \leq \omega_2 \leq \pi\}$

    is mapped to the parallelogram-shaped region

    $\{-\pi \leq 2\omega_1 - \omega_2 \leq \pi\} \cap \{-\pi \leq \omega_1 + \omega_2 \leq \pi\}$

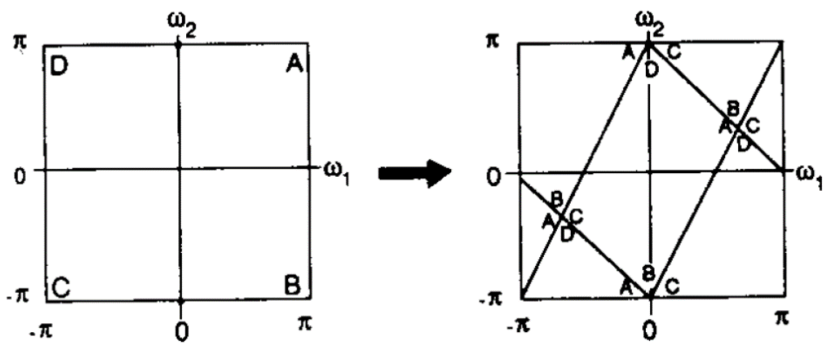

Contourlet

Directional Filter Bank

- **Theorem 2**: (*Multirate identities*) Downsampling by M followed by filtering with a filter $H(\omega)$ is equivalent to filtering with the filter $H(M^T\omega)$ which is obtained by upsampling $H(\omega)$ by M, before downsampling.

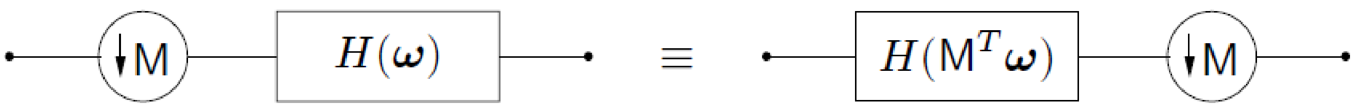

- **Proof:**

$$y_1[n] = x[Mn] * h[n]$$

$$y_2[n] = (x[n] * h_u[n]) \downarrow M = x[Mn] * h[n]$$

$$\Longrightarrow y_1[n] = y_2[n]$$

Contourlet

Directional Filter Bank

- Quincunx sublattice with matrix $Q_0 = \begin{bmatrix} 1 & -1 \\ 1 & 1 \end{bmatrix}, Q_1 = \begin{bmatrix} 1 & 1 \\ -1 & 1 \end{bmatrix}$
  - $|\det(Q_0)| = |\det(Q_1)| = 2,$ one out of two points is retained.

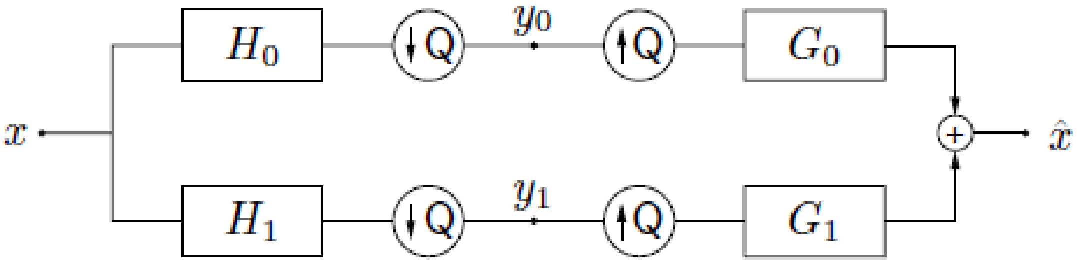

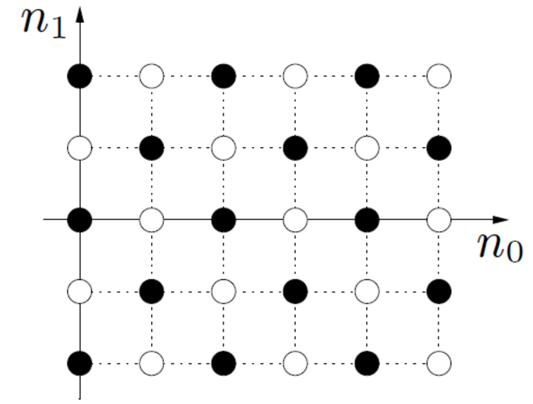

$$\hat{X}(\omega) = \frac{1}{2}[H_0(\omega)G_0(\omega) + H_1(\omega)G_1(\omega)]X(\omega) + \frac{1}{2}[H_0(\omega+\pi)G_0(\omega) + H_1(\omega+\pi)G_1(\omega)]X(\omega+\pi)$$

Contourlet

Directional Filter Bank

- First two levels of Quincunx Filter Bank

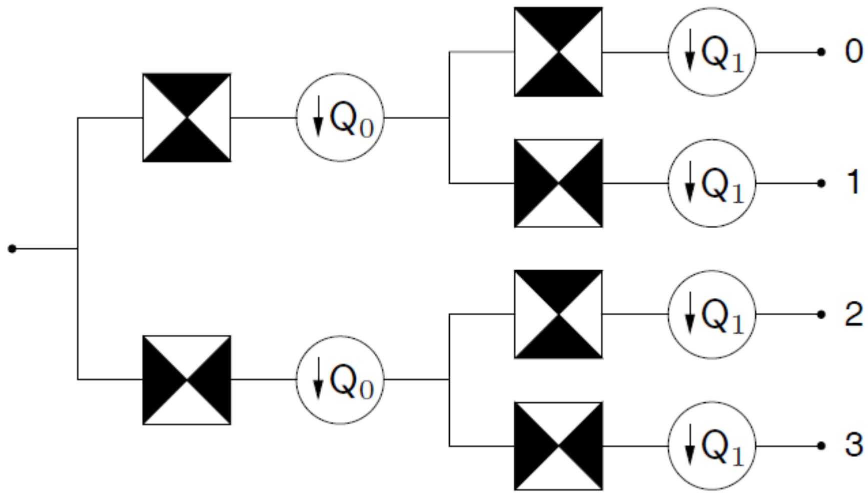

$$Q_0 = \begin{bmatrix} 1 & -1 \\ 1 & 1 \end{bmatrix}$$

$$Q_1 = \begin{bmatrix} 1 & 1 \\ -1 & 1 \end{bmatrix}$$

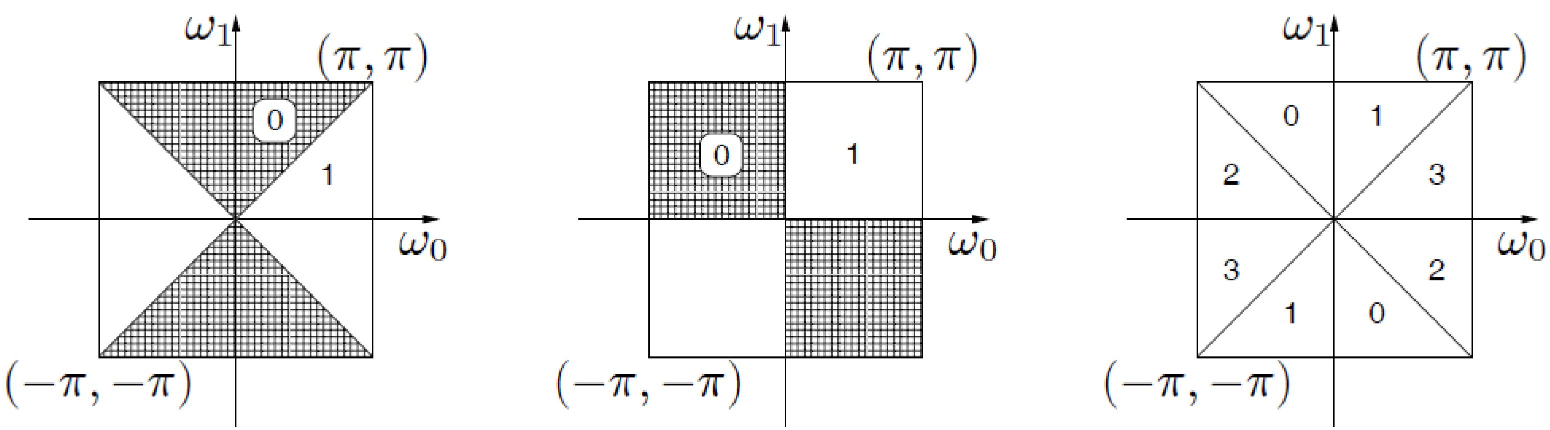

Contourlet

Directional Filter Bank

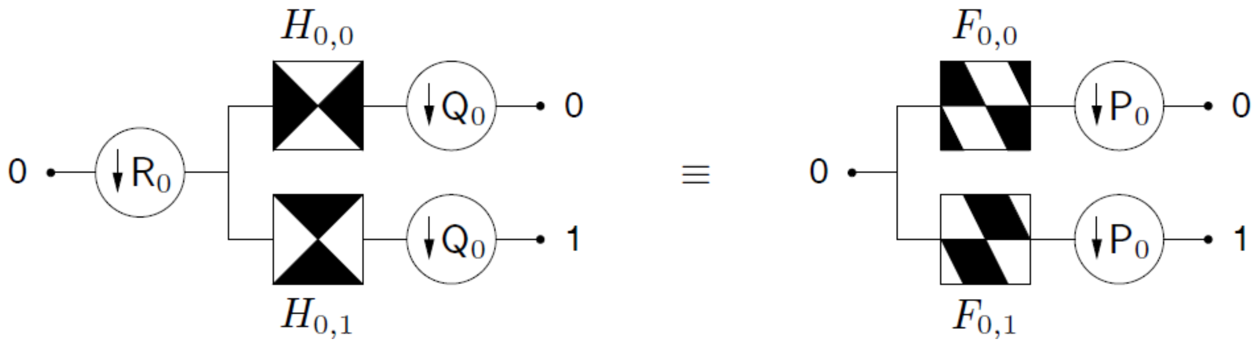

$$R_0 = \begin{bmatrix} 1 & 1 \\ 0 & 1 \end{bmatrix}$$

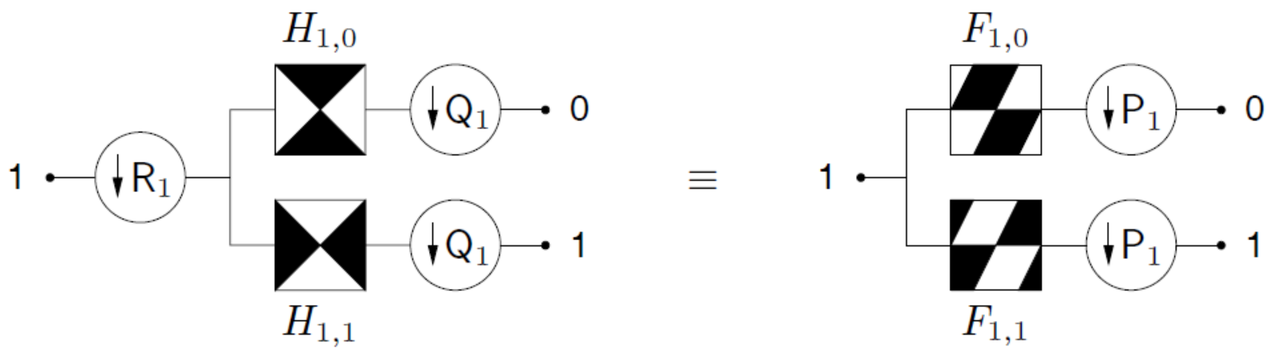

$$R_1 = \begin{bmatrix} 1 & -1 \\ 0 & 1 \end{bmatrix}$$

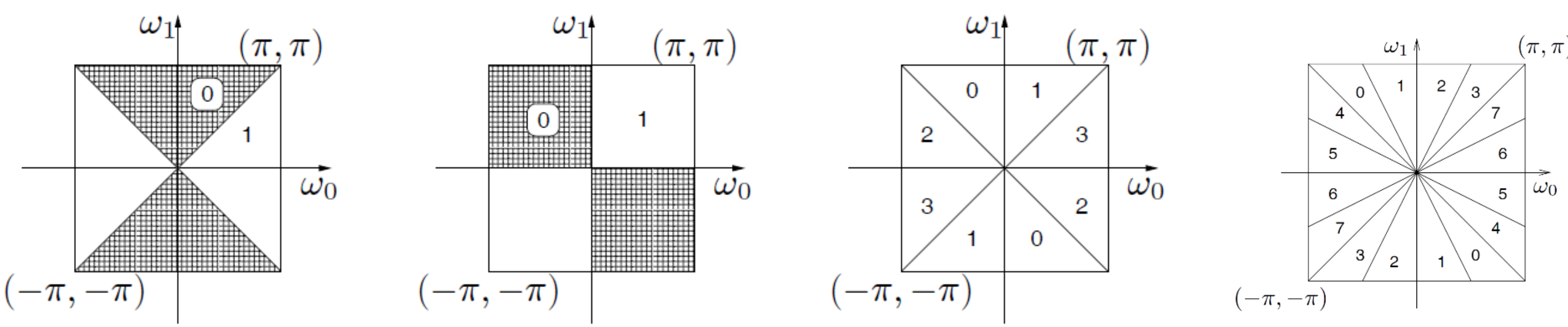

Contourlet

Multiscale

- Under certain regularity conditions, the lowpass synthesis filter in the iterated LP uniquely defines a unique scaling function $\phi(t) \in L_2(R^2)$ that satisfies the following two-scale equation

$$\phi(t) = 2 \sum_{n \in \mathbb{Z}^2} g[n]\phi(2t - n)$$

- $\left\{\phi_{j,n}(t) = \frac{1}{2^j}(t)\phi\left(\frac{t-2^j n}{2^j}\right)\right\}_{n \in \mathbb{Z}^2}$ is an orthonormal basis for approximation subspace $\mathbf{V}_j$ at scale 2^j.

- $\left\{\psi_{j,n}^{(i)}(t) = \frac{1}{2^j}(t)\psi^{(i)}\left(\frac{t-2^j n}{2^j}\right)\right\}_{0 \le i \le 3, n \in \mathbb{Z}^2}$ is a tight frame for $\mathbf{W}_j$

Contourlet

Multiscale

- $\left\{\lambda_{j,n}^{(l)}(t) = \sum_{m\in\mathbb{Z}^2} d_k^{(l)} \frac{1}{2^j}(t)[m - S_k^{(l)} n]\mu_{j,m}(t)\right\}_{n\in\mathbb{Z}^2}$ is a tight frame of a detail directional subspace $\mathbf{W}_{j,k}^{(l)}$

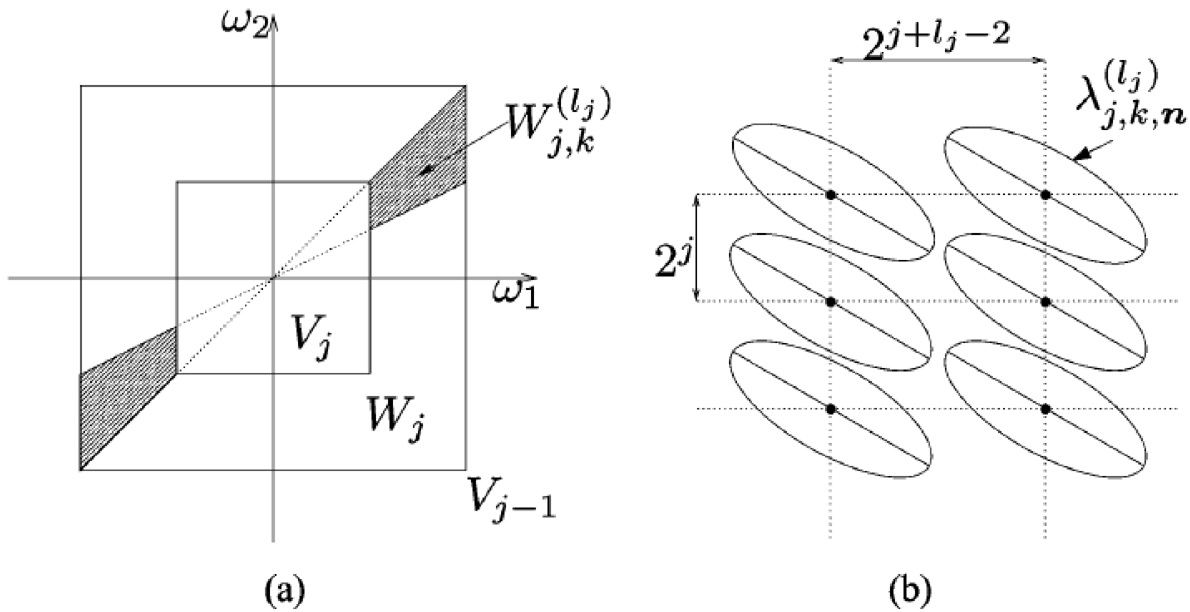

Fig. 9. Contourlet subspaces. (a) Multiscale and multidirection subspaces generated by the contourlet transform which is illustrated on a 2-D spectrum decomposition. (b) Sampling grid and approximate support of contourlet functions for a "mostly horizontal" subspace $W_{j,k}^{(l_j)}$. For "mostly vertical" subspaces, the grid is transposed.

Contourlet

Wavelet Versus Contourlets

- Contourlets offer a much richer set of directions and shapes
- Contourlets are more effective in capturing smooth contours and geometric structures in images.

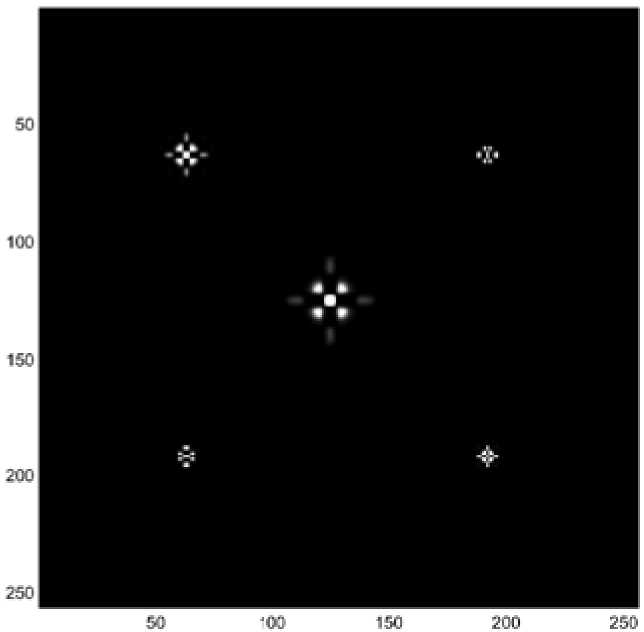

Wavelets

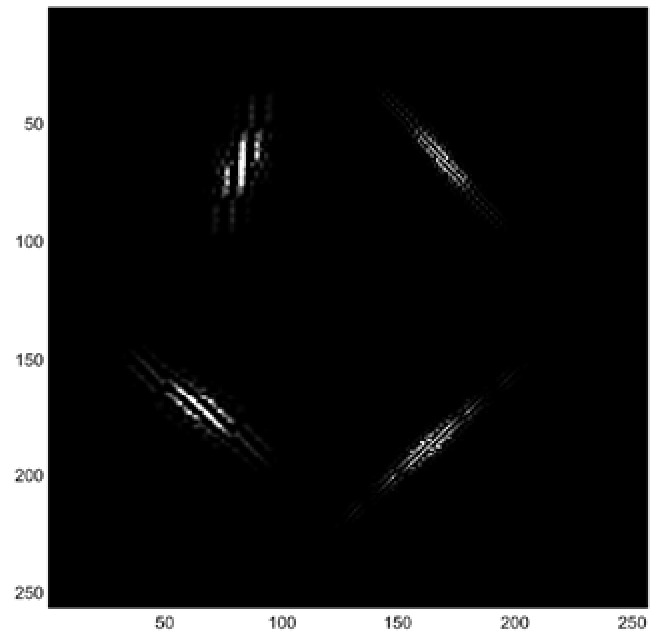

contourlets

Contourlet

Nonlinear approximation

- Nonlinear approximation by the wavelet and contourlet transforms. In each case, the original image Barbara of size 512×512 is reconstructed from the 4096-most significant coefficients. Only part of images are shown for detail comparison.

Original image — Wavelet NLA: PSNR = 24.34 dB — Contourlet NLA: PSNR = 25.70 dB

Contourlet

Denoising

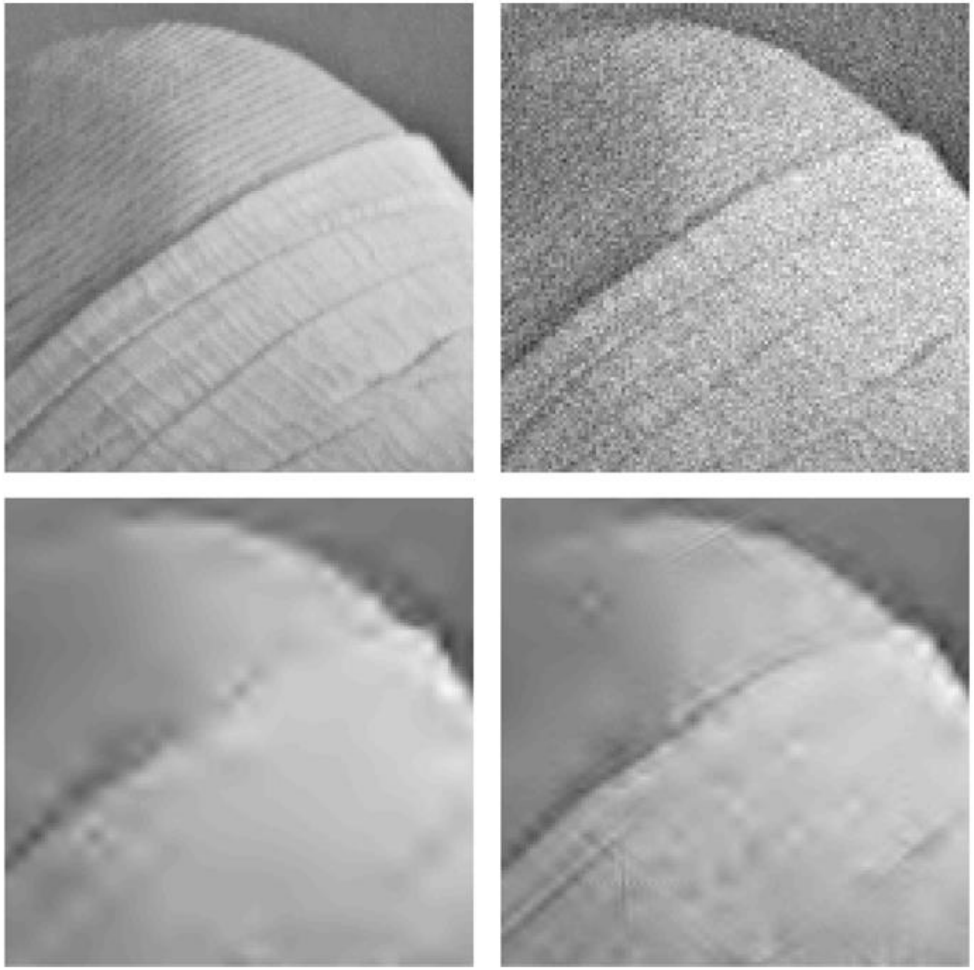

Fig. 17. Denoising experiments. From left to right, top to bottom are: original image, noisy image (PSNR = 24.42 dB), denoising using wavelets (PSNR = 29.41 dB), and denoising using contourlets (PSNR = 30.47 dB).

Contourlet

Properties

- The contourlet expansions are defined on rectangular grids. Its kernel functions cannot be obtained by simply rotating a single function.

- Contourlets have 2-D frequency partition on centric squares, rather than centric circles.

- The contourlet transform has fast filter bank algorithms and convenient tree structures.

- With FIR filters, the iterated contourlet filter bank leads to compactly supported contourlet frames.

Bandelet

Sparse Geometric Image Representation

- Describe the image geometry with a ***geometric flow*** of vectors. These vectors give the local directions in which the image has regular variations.

- Orthogonal bandelet bases are constructed by dividing the image support in regions inside which the geometric flow is parallel.

- Optimized bandelet bases improve significantly image compression and denoisig results obtained with wavelet bases.

- Proposed by Erwan Le Pennec and Stéphane Mallat.

Bandelet

Geometric Flow

- In a region Ω, a geometric flow is a vector field $\vec{\tau}(x_1, x_2)$ which gives a direction in which f has regular variations in the neighborhood of each $(x_1, x_2) \in \Omega$.

- To construct orthogonal bases with the resulting flow, a first regularity condition imposes that the flow is either parallel vertically, which means that $\vec{\tau}(x_1, x_2) = \vec{\tau}(x_1)$, or parallel horizontally and, hence, $\vec{\tau}(x_1, x_2) = \vec{\tau}(x_2)$.

- To maintain enough flexibility, this parallel condition is imposed within subregions Ω_i of the image support. The image support $\mathcal{S}$ is, thus, partitioned into regions $\mathcal{S} = \bigcup_i \Omega_i$, and within each Ω_i the flow is either parallel horizontally or vertically.

Bandelet

Geometric Flow

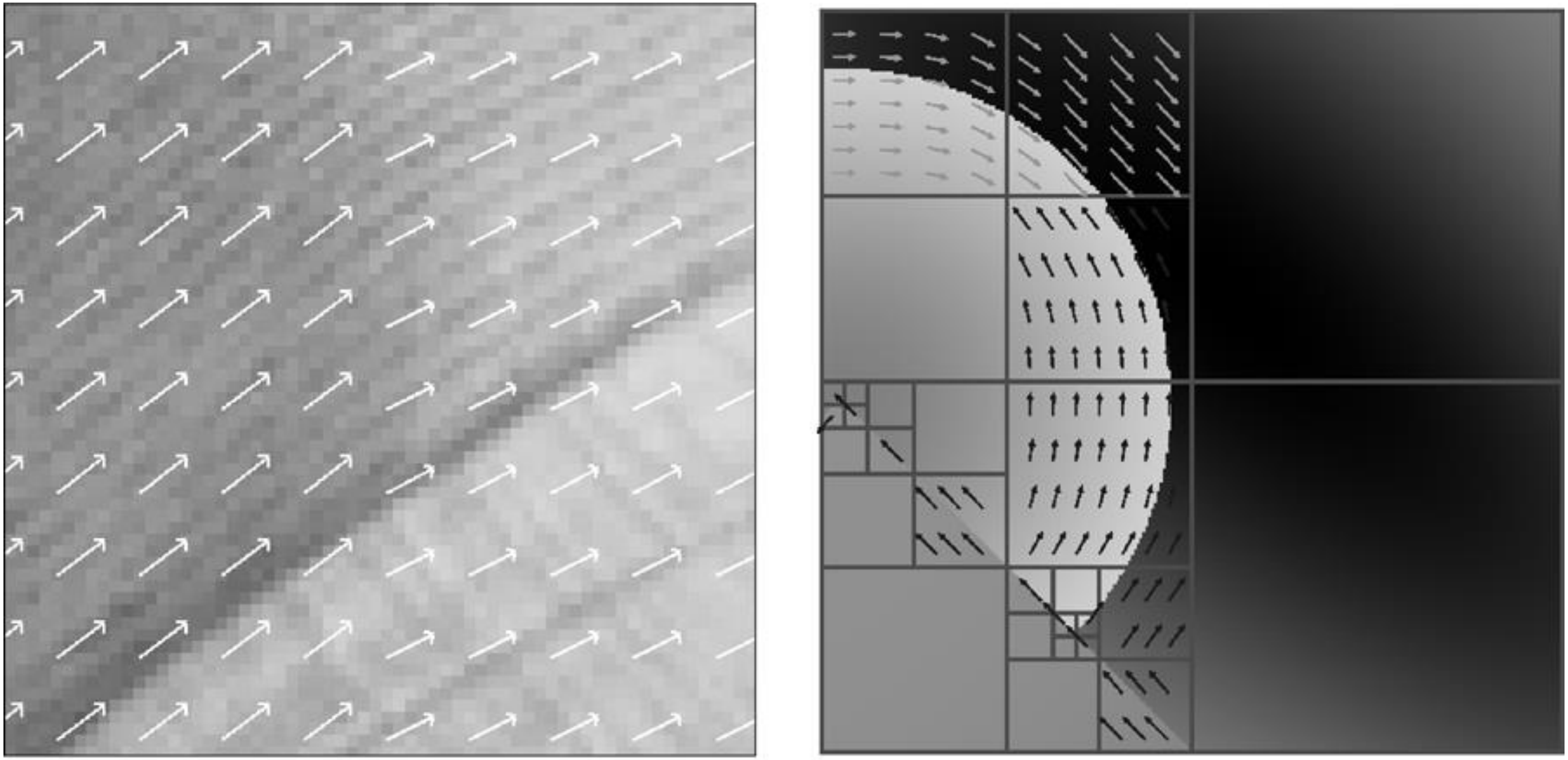

(a) (b)

Fig. (a) Example of flow in a region. Each arrow is a flow vector $\vec{\tau}(x_1, x_2)$. (b) Example of an adapted dyadic squares segmentation of an image and its geometric flow.

Bandelet

Bandeletization

- If there is no geometric flow over a region Ω, which indicates that the image restriction to Ω has an isotropic regularity, then this restriction is approximated in the separable wavelet basis of $\mathbf{L}^{\mathbf{2}}(\Omega)$.

- If a geometric flow is calculated in Ω, this wavelet basis is replaced by a bandelet basis.

- Construct the bandelet basis when the flow is parallel in the vertical direction: $\vec{\tau}(x_1, x_2) = \vec{\tau}(x_1)$.
  - Normalize: $\vec{\tau}(x_1) = \left(1, c'(x_1)\right)$
  - $x_{\min} = \inf_{x_1}\{(x_1, x_2) \in \Omega\}$

- A ***flow line*** is defined as an integral curve of the flow, whose tangents are parallel to $\vec{\tau}(x_1)$.
  - Parallel vertically: a set of point $(x_1, x_2 + c(x_1)) \in \Omega$ for x_1 varying, with $c(x) = \int_{x_{\min}}^{x} c'(u)du$

Bandelet

Bandeletization

- Warpped image: $Wf(x_1, x_2) = f(x_1, x_2 + c(x_1))$.

- $\Psi(x_1, x_2)$ is a wavelet having several vanishing moments along x_1 for each x_2 fixed, then the inner product $\langle Wf, \Psi \rangle = \langle f, \mathrm{W}^* \Psi \rangle$ has a small amplitude.

- W is orthogonal: $W^* f(x_1, x_2) = W^{-1} f(x_1, x_2) = f(x_1, x_2 - c(x_1))$.

- Two equations above suggest decomposing f over a family of ***warped wavelets*** obtained by applying W^{-1} to each wavelet of an orthonormal basis of $\mathbf{L^2}(W\Omega)$.

$$\begin{Bmatrix} \phi_{j,m_1}(x_1)\psi_{j,m_2}(x_2), \\ \psi_{j,m_1}(x_1)\phi_{j,m_2}(x_2), \\ \psi_{j,m_1}(x_1)\psi_{j,m_2}(x_2) \end{Bmatrix}_{j,m_1,m_2 \in \mathbf{I}_{W\Omega}} \xrightarrow{W^{-1}} \begin{Bmatrix} \phi_{j,m_1}(x_1)\psi_{j,m_2}(x_2 - c(x_1)), \\ \psi_{j,m_1}(x_1)\phi_{j,m_2}(x_2 - c(x_1)), \\ \psi_{j,m_1}(x_1)\psi_{j,m_2}(x_2 - c(x_1)) \end{Bmatrix}_{j,m_1,m_2 \in \mathbf{I}_{W\Omega}}$$

an orthonormal basis of $\mathbf{L^2}(W\Omega)$

a warped wavelet orthonormal basis of $\mathbf{L^2}(\Omega)$

Bandelet

Bandeletization

- $\langle f, \mathrm{W}^{-1}\Psi \rangle$ is small if $\Psi(x_1, x_2)$ has vanishing moments along x_1 for each x_2.

$$\left\{\begin{matrix} \phi_{j,m_1}(x_1)\psi_{j,m_2}(x_2), \\ \psi_{j,m_1}(x_1)\phi_{j,m_2}(x_2), \\ \psi_{j,m_1}(x_1)\psi_{j,m_2}(x_2) \end{matrix}\right\}_{j,m_1,m_2\in\mathbf{I}_{W\Omega}}$$

invalid

valid

Because the 1-D wavelet $\psi(t)$ has several vanishing moments, but the scaling function $\phi(t)$ has no vanishing moment.

Necessary to replace the family of orthogonal scaling functions $\{\phi_{j,m_1}(x_1)\}_{m_1}$ by an equivalent family of orthonormal functions, that have vanishing moments.

- The collection of scaling function $\{\phi_{j,m_1}(x_1)\}_{m_1}$ is an orthonormal basis of a multiresolution space which also admits an orthonormal basis of wavelets $\{\psi_{l,m_1}(x_1)\}_{l>j,m_1}$.
- This suggests replacing the orthogonal family $\{\phi_{j,m_1}(x_1)\psi_{j,m_2}(x_2)\}_{j,m_1,m_2}$ by the family $\{\psi_{l,m_1}(x_1)\psi_{j,m_2}(x_2)\}_{j,l>j,m_1,m_2}$. This is called a ***bandeletization***.

Bandelet

Partition

- Divide image into squares of varying dyadic sizes using ***quad tree***

- To represent the image partition with few parameters.
- To be able to compute an optimal partition with a fast algorithm

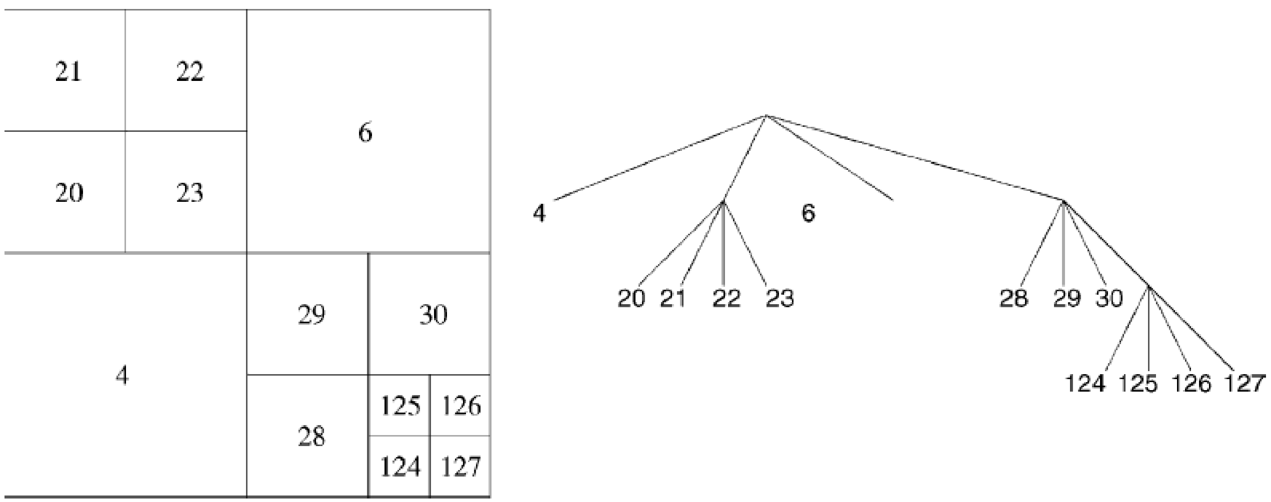

Fig. Example of dyadic square image segmentation. Each leaf of the corresponding quad tree corresponds to a square region having the same index number.

Bandelet

Optimization

- Best approximation – minimize the approximation error $\|f - f_M\|$
  - $M = M_G + M_B$
  - M_G - number of parameters define a block bandelet basis constructed over this partition
  - M_B - number of bandelet coefficients above threshold T (f_M is reconstructed from these coefficients)

- Find a best bandelet basis that minimizes the Lagrangian

$$\mathcal{L}(f, T) = \|f - f_M\|^2 + T^2 M$$

- Suppose that the image has contours that are C^α curves which meet at corners or junctions, and that is C^α away from these curves.

- Optimal asymptotic error decay rate

$$\|f - f_M\|^2 \le C M^{-\alpha}$$

Bandelet

Nonlinear approximation

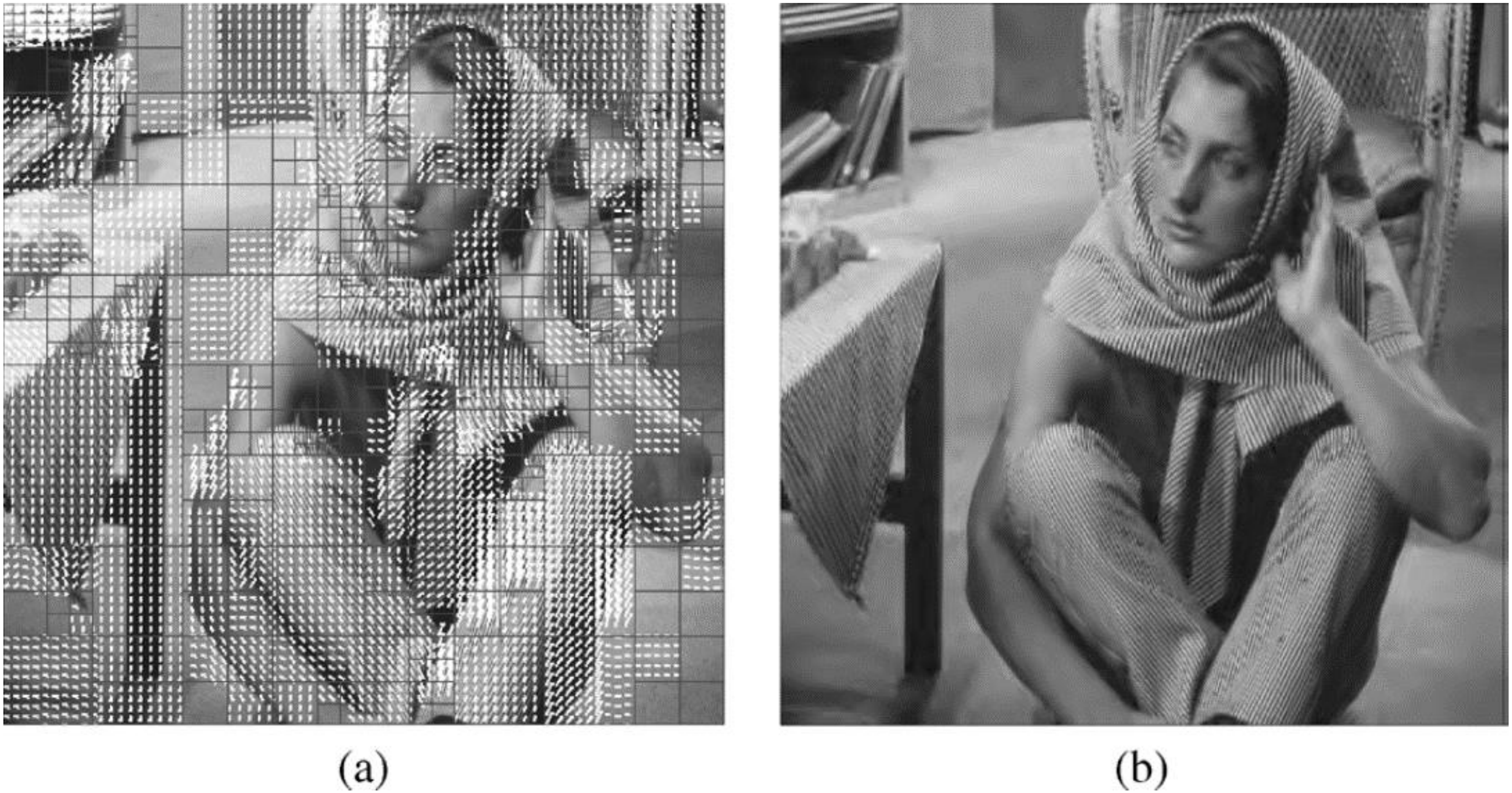

Fig. (a) Geometric flow segmentation obtained for Barbara and $R = 0.44$ bits/pixel. (b) The bandelet reconstruction with a PSNR of 31.3 dB.

Bandelet

Nonlinear approximation

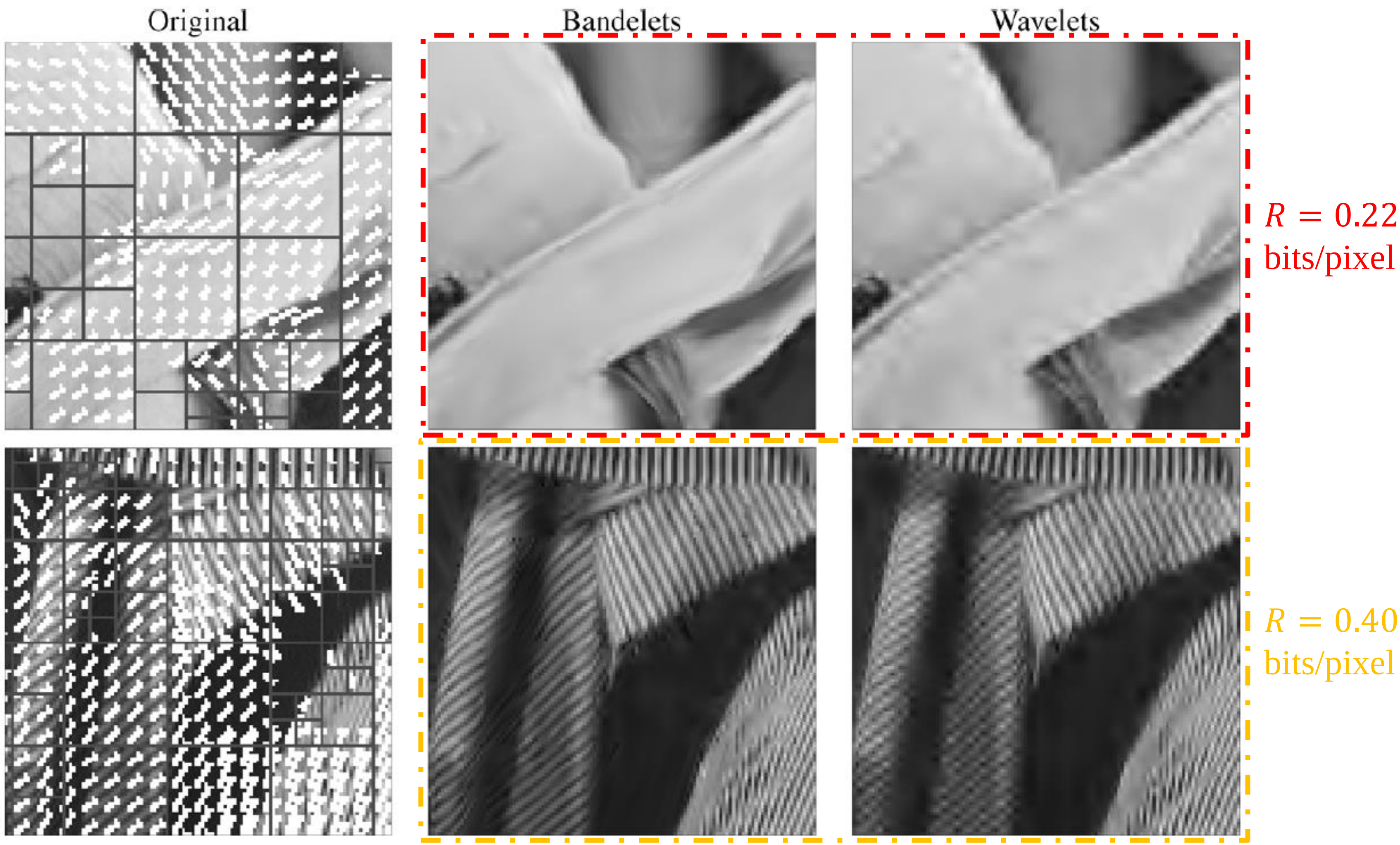

Bandelet

Denoising

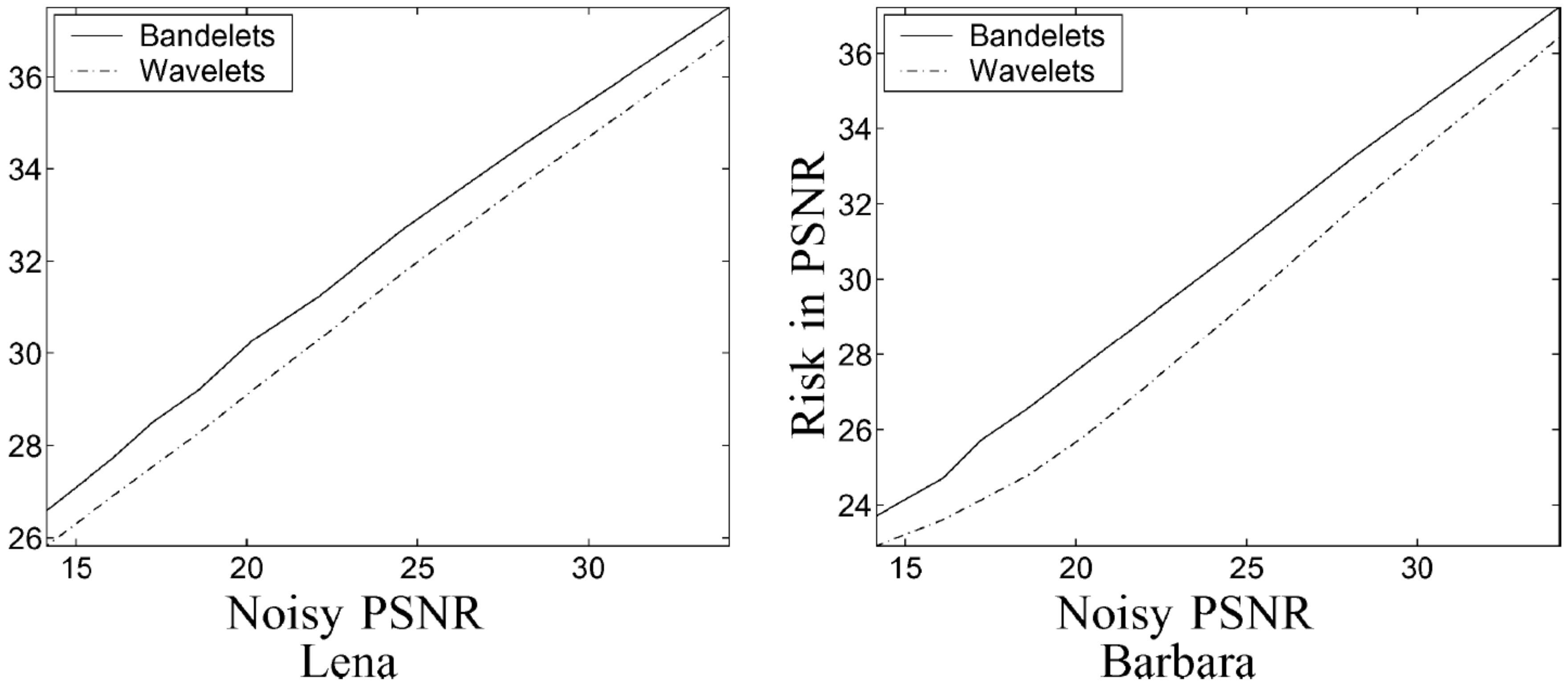

Fig. Risk in PSNR of (full lines) the bandelet thresholding estimator and of (dashed lines) the wavelet thresholding estimator for the Lena and Barbara images as a function of the PSNR of the original noisy signal. The bandelet estimator reduces the risk by approximatively 1 dB for Lena and by 1.8 dB for Barbara.

Bandelet

Denoising

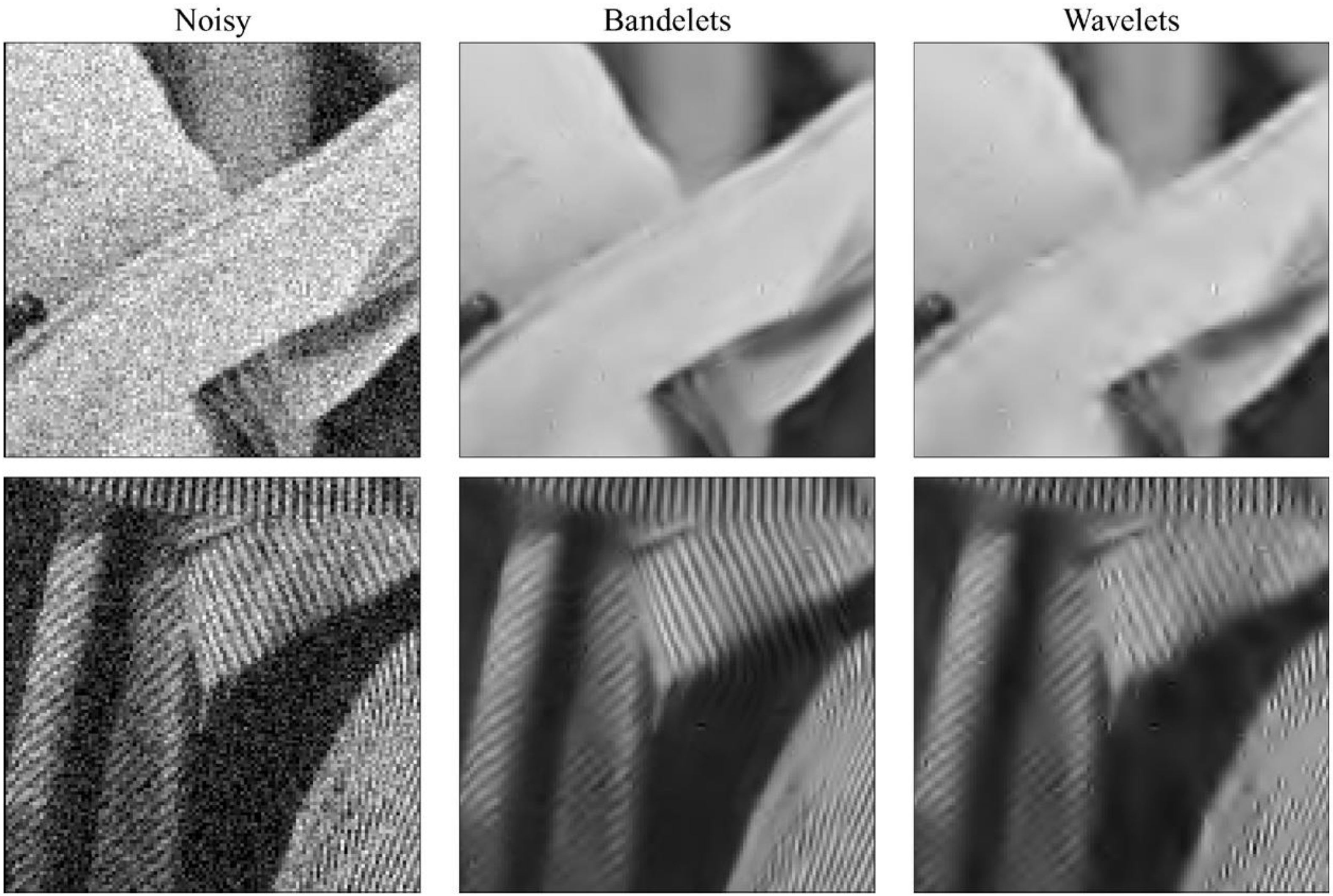

Institute of Media,
Information, and Network

Q & A

Many Thanks